

2025



CONTRIBUTION OF DIFFERENTIAL

EQUATIONS TO THE
SUPPLY CHAIN



Oleh:
Dr. Muh. Deni Johansyah , Drs., M.M.

CONTRIBUTION OF DIFFERENTIAL EQUATIONS TO THE SUPPLY CHAIN

Penyusun

Dr. Muh. Deni Johansyah , Drs., M.M



CONTRIBUTION OF DIFFERENTIAL EQUATIONS TO THE SUPPLY CHAIN

Copyright © 2025 pada Penulis

ISBN: -

Penulis:

Dr. Muh. Deni Johansyah , Drs., M.M

Diterbitkan pertama kali oleh:

Unibi Press

Anggota IKAPI, Jawa Barat, 2021

Jl. Soekarno Hatta no. 643, Bandung, Jawa Barat 40285

Tlp./SMS/Whatsapp : 0812-222-881-89

unibipress@unibi.ac.id

Hak cipta dilindungi undang–undang. Dilarang memperbanyak atau memindahkan sebagian atau seluruh isi buku ke dalam bentuk apapun, secara elektronik maupun mekanis, termasuk fotokopi, merekam, atau dengan teknik perekaman lainnya tanpa seizin tertulis dari penerbit. Undang-undang Nomor 28 Tahun 2014 tentang Hak Cipta

CHAPTER 1

Dynamical Analysis and Sliding Mode Controller for the New 4D Chaotic Supply Chain Model based on the Product Received by Customer

1.1 Introduction

1.2 New 4-D Chaotic Supply Chain Model (4D CSCM)

1.3 Dynamical Analysis

1.3.1. Influence of parameter "a" on system's behavior

1.3.2. Influence of parameter "b" on system's behavior

1.3.3. Influence of parameter "c" on system's behavior

1.3.4. Influence of parameter "d" on system's behavior

1.3.5. Influence of parameter "p" on system's behavior

1.3.6. Influence of initial conditions on system's behavior

1.4 Sliding Mode Controller

1.5 Conclusion

1.6 References

CHAPTER 2

Enhanced Chaotic Modeling of Supply Chains with Market Shock and Intelligent Fuzzy Control

2.1 Introduction

2.2 Model of N5DCSCM

2.3 Dynamic Analysis

2.3.1 Multistability Analysis

2.3.2 Complete Amplitude Control via Rescaling

2.3.3 Offset Boosting Control

2.4 Fuzzy logic-based controller design

2.5 Numerical simulations

2.6 Conclusion

2.7 References

CHAPTER 3

Controlling the Unpredictable: Bifurcation and Backstepping Strategies in Supply Chain Dynamics

3.1 Introduction

3.2 A Chaotic Supply Chain Model

3.3 Dynamical Analysis

3.4 Parameter a varying

3.5 Parameter b varying

3.6 Complete Synchronization of Chaotic SCMM using Backstepping Control

3.7 Conclusion

3.8 References

CHAPTER 1

Dynamical Analysis and Sliding Mode Controller for the New 4D Chaotic Supply Chain Model based on the Product Received by Customer

1.1 Introduction

Initially, supply chain management focused on linear and deterministic models to optimize operations [1,2]. However, as businesses encountered increasing complexity and unpredictability, researchers began to recognize the limitations of these traditional approaches. Chaos theory provided a framework for understanding the nonlinear dynamics and emergent behaviors inherent in supply chain systems [3,4]. Studies identified chaotic behavior in various aspects of supply chain operations, including demand forecasting [5], inventory management [6], production scheduling [7], and distribution logistics [8]. These findings highlighted the need for new methodologies capable of managing and controlling the inherent chaos within supply chains [9,10].

In addressing the intricacies of supply chains, certain academics have utilized nonlinear dynamics theory to investigate pertinent issues. [11] introduced a pricing game model for a closed-loop supply chain system, involving a manufacturer and a retailer with distinct rationalities. [12] analyzed a three-dimensional mathematical model of supply chains, with the goal of stabilizing chaotic behavior. This involved introducing a linear control parameter to manage production levels and mitigate the risk of potential collapse, which could lead to dangerous instability. [13] explored the emergence of chaos within multi-level supply chains and provided insights into managing relevant factors to mitigate or eliminate system chaos. [14] investigated the dynamic behavior of a three-tier supply chain and devised an adaptive algorithm to counteract irregular dynamics stemming from uncertainties. [15] proposed a novel supply chain model considering non-monotonic demand variations with inventory levels and discussed synchronization phenomena in coupled supply chain models under both unidirectional and bidirectional coupling. [16] addressed the synchronization issue in supply chain systems using an active and adaptive integral sliding mode control method. Despite the existing literature, there remains limited discourse on dynamical analysis in 4D supply chain management. Thus, further research is warranted to explore studies concerning supply chains in 4D systems.

Chaos control associated with complex phenomena has been identified in actual supply chain systems. Numerous researchers have explored control and synchronization methods to characterize these systems in the literature such as robust control [9], delayed feedback control [17], adaptive sliding mode control [18], ANN [19], ANFIS [20], Robust H^∞ control [21], tracking control [22], stochastic fixed-time tracking control [23], fuzzy neural network control [24] and nonlinear control [25].

Studying the SMC for the new 4D CSCM based on the product received by the customer is important because it enhances the stability and control of complex, nonlinear supply chain behaviors, ensuring smooth and predictable operations [26]. The SMC effectively mitigates risks such as transportation delays, quality fluctuations, and information distortion by dynamically adjusting system parameters, reducing disruptions [27]. This leads to improved supply chain performance, including better inventory management, reduced lead times, and optimized resource utilization, resulting in increased efficiency and cost savings. The controller's adaptability to real-time changes ensures the supply chain remains resilient in the face of unexpected fluctuations. Additionally, the SMC manages coexisting attractors, steering the system towards desirable states and avoiding undesirable outcomes. Practical applications of the SMC translate into better forecasting, inventory control, and risk management, maintaining competitive advantage [28]. This study bridges the gap between advanced control theory and practical supply chain dynamics, providing valuable insights and opening new avenues for research and application. The validation of the SMC through simulations demonstrates its potential in handling complex supply chain issues and provides confidence in its practical deployment.

In the dynamic landscape of supply chain management, the emergence of chaos theory has shed light on the complex and unpredictable behavior inherent in supply chain systems. With the recognition of chaotic dynamics within supply chains, there arises a need to explore novel control strategies capable of navigating this intricate environment effectively. This project focuses on addressing this challenge through the development of a sliding mode controller for a new 4D CSCM, specifically centered on the product received by the customer.

The integration of chaos theory into supply chain dynamics underscores the existence of coexisting attractors. Understanding and controlling these attractors are crucial for ensuring stability and optimizing performance in supply chain operations. By leveraging the insights from chaos theory and employing advanced control techniques such as sliding mode control, this project aims to design a control framework capable of managing the complex dynamics of the supply chain model.

The main contribution and novelty of this paper include investigating the dynamics of the new 4D CSCM based on the product received by the customer, identifying and characterizing coexisting attractors within the supply chain system, developing a sliding mode control strategy to regulate the system dynamics and stabilize the supply chain operation, and evaluating the performance and efficacy of the proposed sliding mode controller through simulation and validation studies.

This work is systematized as follows. The next section presents the introduction and objectives of the study. In Section 2, we derive the new 4D CSCM based on the product received by the customer. Section 3 investigates the dynamical behavior of the proposed system, examining the influence of different parameters through techniques such as Lyapunov exponents spectrum, bifurcation diagrams, and phase plots. Furthermore, in Section 4, we propose a sliding mode control strategy for the new 4D CSCM, deriving the equivalent control law and validating

its effectiveness through simulation studies. The study is summarized and concluding remarks are presented in the final section.

1.2 New 4-D Chaotic Supply Chain Model (4D CSCM)

Supply chains are complex systems involving multiple interconnected components such as suppliers, manufacturers, distributors, retailers, and customers [29]. These components interact dynamically, with various factors influencing the overall performance and stability of the supply chain [30]. Traditional models have often been inadequate in capturing the inherent nonlinearities and chaotic behavior present in real-world supply chains. To address this, recent studies have focused on developing models that can better represent these complexities. One such model is the four-dimensional (4D) chaotic supply chain model, which extends the conventional three-dimensional models by incorporating an additional dimension.

Cuong et al. [31] described a four-tier integrated chaotic supply chain model, which can be represented by a system of differential equations. This model considers the interactions between product demand at a retailer, the quantity of product supplied by the distributor, the product produced by the manufacturer, and the product received by the customer. By incorporating various risk factors such as transportation risk, quality risk, distortion, contingency reserves, and safety stock, the model aims to provide a more realistic representation of supply chain dynamics. The four-tier integrated chaotic supply chain model by the following 4-D system of differential equations:

$$\begin{cases} \dot{x} = ay - (m + 1)x + dw \\ \dot{y} = cx - xz - y \\ \dot{z} = xy - bz \\ \dot{w} = -x - (m + 1)w \end{cases} \quad (1)$$

where x is product demand at a retailer, y is quantity of product that the distributor can supply, z is the product produced at a manufacturer and w is the product received by the customer. Moreover, in the chaotic supply chain model (1), we include various coefficients such that of transport risk a , quality risk b , distortion c , contingency reserve d and safety stock m between customer and retailer

When $a = m + 1$, the chaotic supply chain system (1) reduces to the 4-D Lorenz-Stenflo system given by the dynamics

$$\begin{cases} \dot{x} = a(y - x) + dw \\ \dot{y} = cx - xz - y \\ \dot{z} = xy - bz \\ \dot{w} = -x - aw \end{cases} \quad (2)$$

When $a = 2, b = 1.05, c = 26$ and $d = 1.5$, witnessed a chaotic attractor exhibited by the 4-D CSCM (2) for the initial values $x(0) = y(0) = z(0) = w(0) =$

0.04. In fact, for $T = 1E4$ seconds, the Lyapunov exponents for the Cuong system (2) were found to be:

$$L_1 = 0.4228, L_2 = 0, \quad (3)$$

$$L_3 = -2.9262,$$

$$L_4 = -3.5468$$

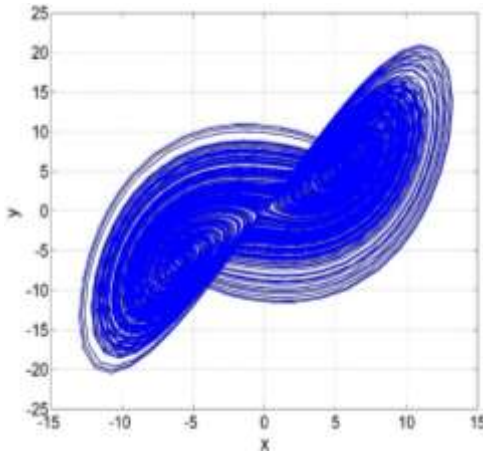
This paper proposes a new chaotic supply chain system by adding a quadratic nonlinear term px^2 in the third differential equation of the Cuong chaotic system (2). Thus, our new 4-D chaotic supply chain system can be modelled according to a system of differential equations:

$$\begin{cases} \dot{x} = a(y - x) + dw \\ \dot{y} = cx - xz - y \\ \dot{z} = xy - bz + px^2 \\ \dot{w} = -x - aw \end{cases} \quad (4)$$

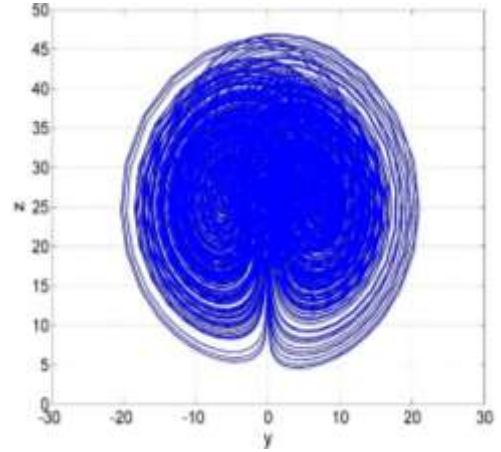
We take new values for the system parameters as $a = 5.5, b = 1.8, c = 27, d = 1.6$ and $p = 0.5$. We take the initial values of the system (4) as $x(0) = 0.04, y(0) = 0.04, z(0) = 0.04$ and $w(0) = 0.04$. For $T = 1E4$ seconds, we calculated the Lyapunov exponents for the new 4-D system (4) and obtained the following:

$$L_1 = 0.8006, L_2 = 0, L_3 = -5.8404, L_4 = -8.7601. \quad (4)$$

We notice the positive Lyapunov exponent of the new chaotic supply chain system (4) is significantly greater than that of Cuong chaotic system (2). This implies that the new 4D CSCM (4) exhibits more complexity than the Cuong chaotic system (2). The phase portrait of the new 4D CSCM (4) can be seen in Figure 1.



(a)



(b)

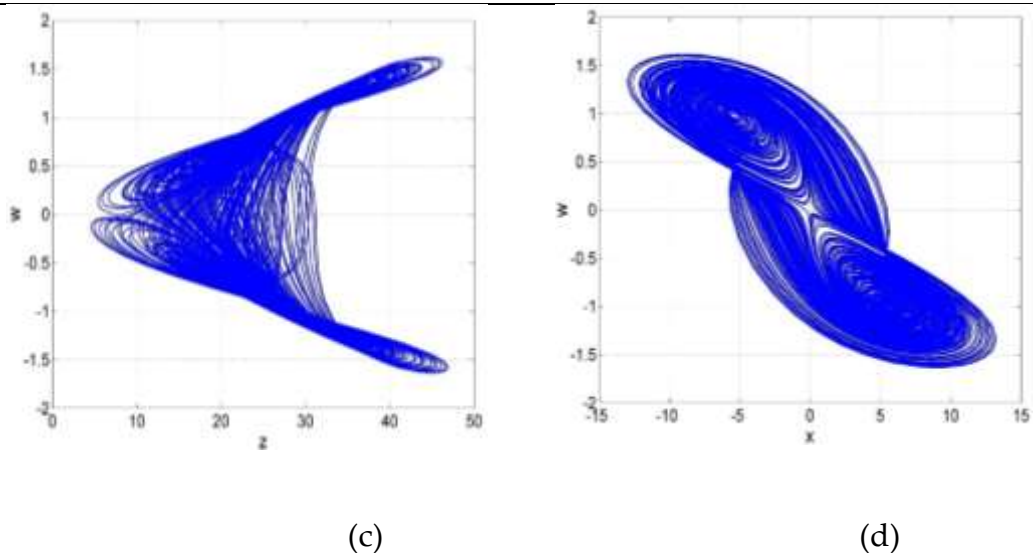


Figure 1. MATLAB simulation for the system (4): (a) x-y plane, (b) y-z plane, (c) z-w plane and x-w plane.

1.3 Dynamical Analysis

In this section, we explore a detailed examination of how the proposed system behaves, looking closely at how its parameters and initial conditions interact. Using various crucial techniques like Lyapunov exponents spectrum, bifurcation diagrams, and phase plots, we uncover how the system behaves, pinpointing areas of chaos, multistability, and other interesting phenomena. As explained further, our analysis reveals that the system is capable of producing chaotic behavior, with a maximum Lyapunov exponent of 1.48. Additionally, we discover the occurrence of multistability, providing a clear picture of its effects.

13.1. Influence of parameter "a" on system's behavior

This subsection investigates the influence of parameter 'a' in shaping the behavior of the proposed system. By systematically varying parameter 'a' within the range of [5, 20], we explore its impact on the system's dynamics. Through the bifurcation diagram and Lyapunov exponents spectrum shown in Figures 2(a) and 2(b) respectively, we demonstrate that System (4) can exhibit chaotic and periodic behaviors for specific intervals of parameter 'a'.

When $5 < a < 15.3$, System (4) exhibits chaotic behavior, as demonstrated by Figure 2(a). Additionally, Figure 2(b) clearly illustrates that the Maximum Lyapunov Exponent (MLE) is positive within this range. Furthermore, we observe windows of periodic behaviors nestled between chaotic regions at specific values of 'a,' namely ([9.5, 9.6], [10.1, 10.15], [11.31, 11.34], [13.6, 13.9]). For enhanced clarity, we provide a visualization of the chaotic attractor in Figure 2(c) for the case when $a = 6$. The resulting Lyapunov Exponents according to this setting are: $LE1 = 0.812$, $LE2 = 0$, $LE3 = -6.338$, and $LE4 = -9.275$.

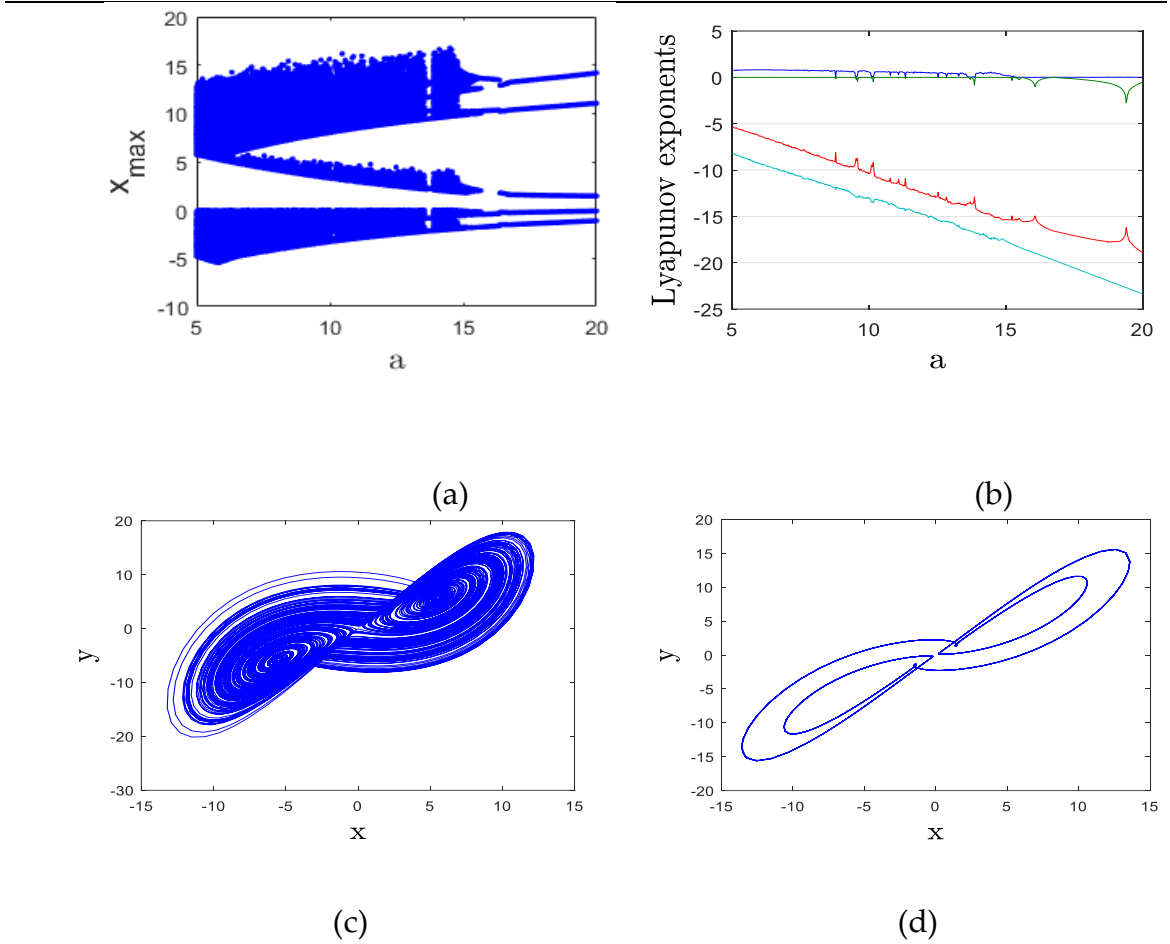


Figure 2. Chaotic exhibition of system (4): (a) bifurcation diagram, (b) Lyapunov exponents, (c) x-y chaotic attractor for $a=6$, (d) x-y periodic attractor for $a=18$.

When $15.3 < a < 20$, System (4) demonstrates periodic behavior, as illustrated in Figure 2(a). Furthermore, Figure 2(b) highlights that the Maximum Lyapunov Exponent (MLE) is zero within this interval. Additionally, for further insight, we present a visualization of the periodic attractor in Figure 2(d) corresponding to the case when $a = 18$. The resulting Lyapunov Exponents according to this setting are: $LE1 = 0$, $LE2 = -0.293$, $LE3 = -17.386$, and $LE4 = -21.123$.

Transportation risk is a significant factor in supply chain management, influencing the stability and performance of the entire system [32]. By varying the transportation risk parameter in our 4D CSCM. Chaotic behavior in the supply chain due to transportation risk can be identified by irregular and unpredictable fluctuations in inventory levels, order quantities, and delivery schedules. This erratic behavior is often caused by factors such as delays, disruptions, and variability in transportation times. Periodic behavior, on the other hand, is characterized by regular, repeating patterns in the supply chain dynamics. This occurs when the transportation risk is more predictable and stable, leading to consistent and cyclical patterns in inventory and order levels.

1.3.2. Influence of parameter "b" on system's behavior

In this subsection, we explore the influence of parameter 'b' on the behavior of the system (4) by systematically varying it within the range of $[0, 2]$. This observation was based on the dynamics of bifurcation diagram and Lyapunov exponents spectrum.

For $0 < b < 0.51$, System (4) demonstrates periodic behavior, as depicted in Figure 3(a). Notably, Figure 3(b) reveals that the Maximum Lyapunov Exponent (MLE) is zero within this range. Furthermore, we observe intervals of chaotic behavior amidst periodic regions at specific values of 'b,' namely $([0.03, 0.07], [0.1, 0.13], [0.18, 0.20], [0.22, 0.25])$. Figure 3(c) illustrates the periodic attractor for the case when $b = 0.3$. The resulting Lyapunov Exponents according to this setting are: $LE1 = 0$, $LE2 = -0.349$, $LE3 = -4.756$, and $LE4 = -7.201$.

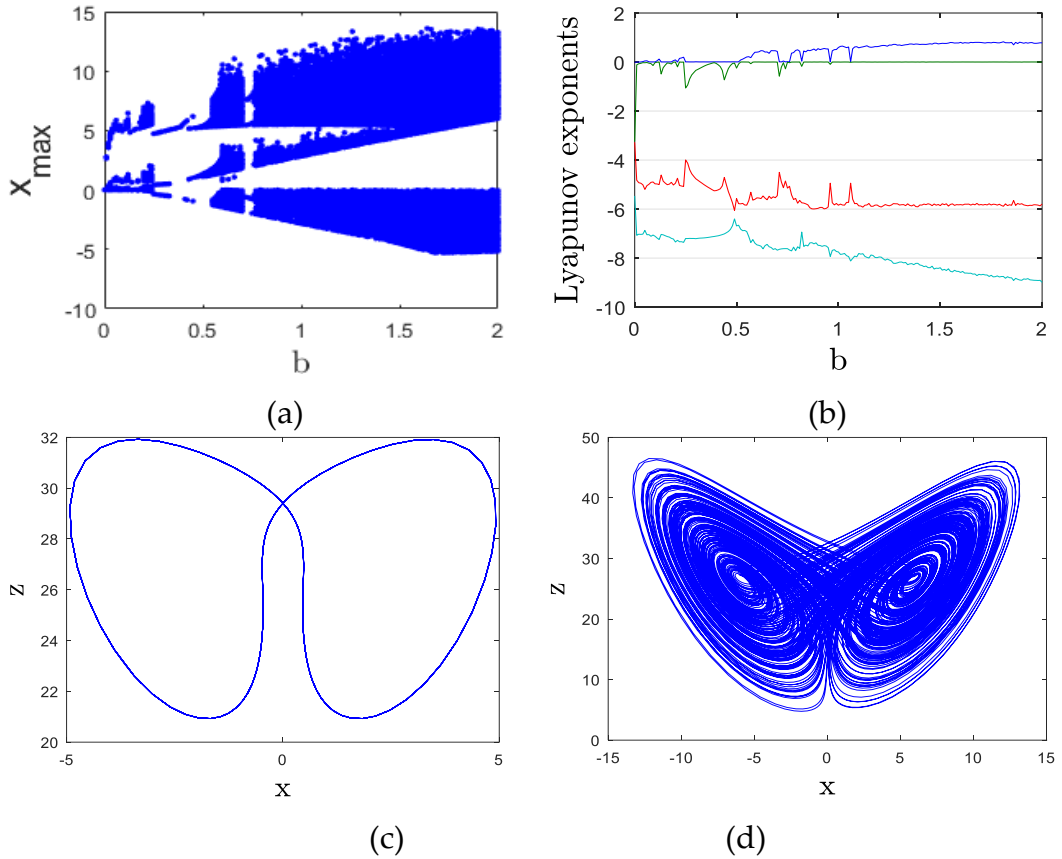


Figure 3. Chaotic exhibition of system (4): (a) bifurcation diagram, (b) Lyapunov exponents, (c) x-z periodic attractor for $b=0.3$, (d) x-z chaotic attractor for $b=2$.

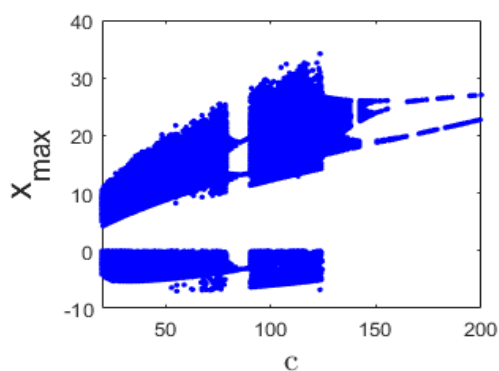
For $0.51 < b < 2$, System (4) exhibits chaotic behavior, except for the intervals when $b = [0.71, 0.76]$, $b = 0.82$, and $b = 0.96$, where it demonstrates periodic behavior, as found in Figure 3(a). Additionally, Figure 3(b) gives an indication of positive MLE within this range. To provide further insight, we present a visualization of the chaotic attractor in Figure 3(d) corresponding to the case when $b = 2$. The resulting Lyapunov Exponents according to this setting are: $LE1 = 0.789$, $LE2 = 0$, $LE3 = -5.814$, and $LE4 = -8.975$.

Chaotic behavior due to quality risk is characterized by unpredictable fluctuations in product quality, leading to erratic order quantities, inventory levels, and customer satisfaction [33]. Factors contributing to chaotic behavior include inconsistent production processes, supplier quality issues, and variable inspection standards. In the chaotic regime, phase portraits of supply chain variables (e.g., product quality vs. inventory level) show intricate, non-repeating patterns, indicating high sensitivity to initial conditions. Small changes in quality risk can lead to significantly different outcomes, highlighting the unpredictable nature of the system. Periodic behavior, in contrast, is characterized by regular, repeating patterns in the supply chain dynamics due to stable and predictable product quality. This occurs when quality risk is minimized through consistent production processes and reliable suppliers. In the periodic regime, phase portraits show closed, repeating loops, indicating stable and predictable behavior. Periodic behavior allows for consistent product quality, enhancing customer satisfaction and reducing the need for returns or rework.

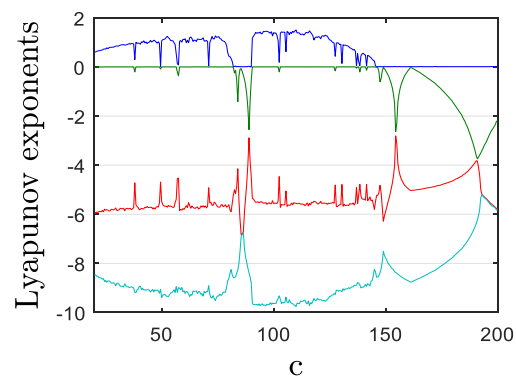
1.3.3. Influence of parameter "c" on system's behavior

This subsection examines the effect of systematically varying parameter 'c' on the system's behavior within the range of [20, 200]. This observation was drawn from the dynamics of the bifurcation diagram and Lyapunov exponents spectrum.

For the interval of c ([20, 82], [90, 145.5]), System (4) displays chaotic behavior, with exceptions noted when $c = [57, 57.5]$, $c = 49.5$, $c = 197$, $c = 138.5$, and $c = 141.5$, where it exhibits periodic behavior, as shown in Figure 4(a). Moreover, Figure 4(b) indicates a positive Maximum Lyapunov Exponent (MLE) within this range. To offer deeper insight, we provide a visualization of the chaotic attractor in Figure 4(c) corresponding to the case when $c = 110$. The resulting Lyapunov Exponents according to this setting are: $LE1 = 1.482$, $LE2 = 0$, $LE3 = -5.572$, and $LE4 = -9.710$.



(a)



(b)

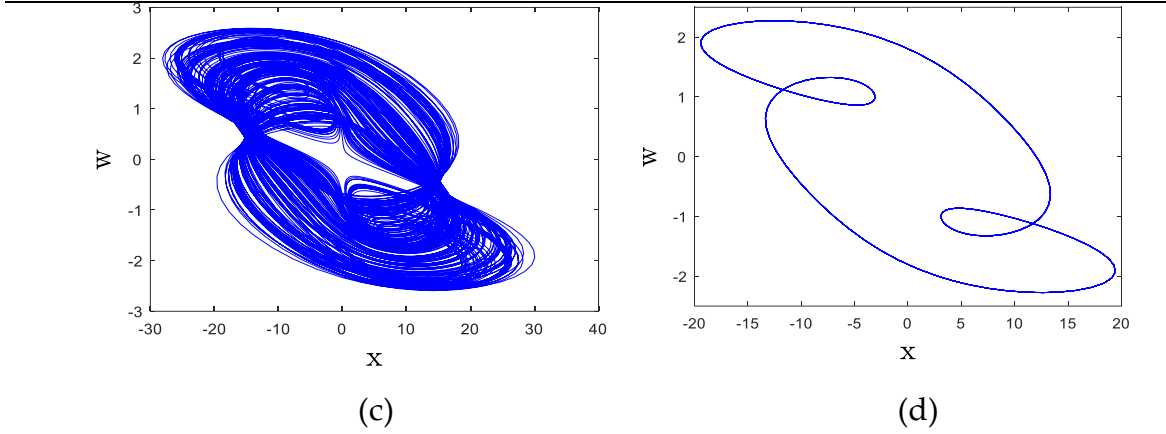


Figure 4. Chaotic exhibition of system (4): (a) bifurcation diagram, (b) Lyapunov exponents, (c) x-w chaotic attractor for $c=110$, (d) x-w periodic attractor for $c=89$.

For the range of c ($[92, 90]$, $[145.5, 200]$), System (4) demonstrates periodic behavior, as illustrated in Figure 4(a). Notably, Figure 4(b) reveals that the MLE is zero within this interval. Figure 4(d) illustrates the periodic attractor for the case when $c = 89$. The resulting Lyapunov Exponents according to this setting are: $LE1 = 0$, $LE2 = -2.591$, $LE3 = -2.849$, and $LE4 = -8.373$.

Distortion in supply chain management refers to discrepancies and inaccuracies in information flow, demand forecasts, and order quantities, often leading to the well-known "bullwhip effect" [34]-[35]. In the chaotic regime, phase portraits of supply chain variables (e.g., order quantity vs. inventory level) show complex, non-repeating patterns, indicating high sensitivity to initial conditions. Small changes in distortion can lead to significantly different outcomes, highlighting the unpredictable nature of the system. Periodic behavior, in contrast, is characterized by regular, repeating patterns in the supply chain dynamics due to accurate and timely information flow. This occurs when distortion is minimized through synchronized communication and reliable data analytics.

1.3.4. Influence of parameter "d" on system's behavior

In this subsection, we explore the impact of parameter 'd' on the system's behavior by systematically varying it within the range of $[-35, 5]$. This observation was drawn from the dynamics of the bifurcation diagram and Lyapunov exponents spectrum.

For the interval of d ($[-35, -25.5]$, $[-22.8, -20.2]$), System (4) predominantly exhibits periodic behavior, except for the subrange of d $[-20.7, -20.45]$, where chaos emerges, as found in Figure 5(a). Notably, Figure 5(b) suggests a zero Maximum Lyapunov Exponent (MLE) within this interval. Figure 5(c) illustrates the periodic attractor for the case when $d = -27$. The resulting Lyapunov Exponents according to this setting are: $LE1 = 0$, $LE2 = -0.468$, $LE3 = -0.499$, and $LE4 = -12.841$.

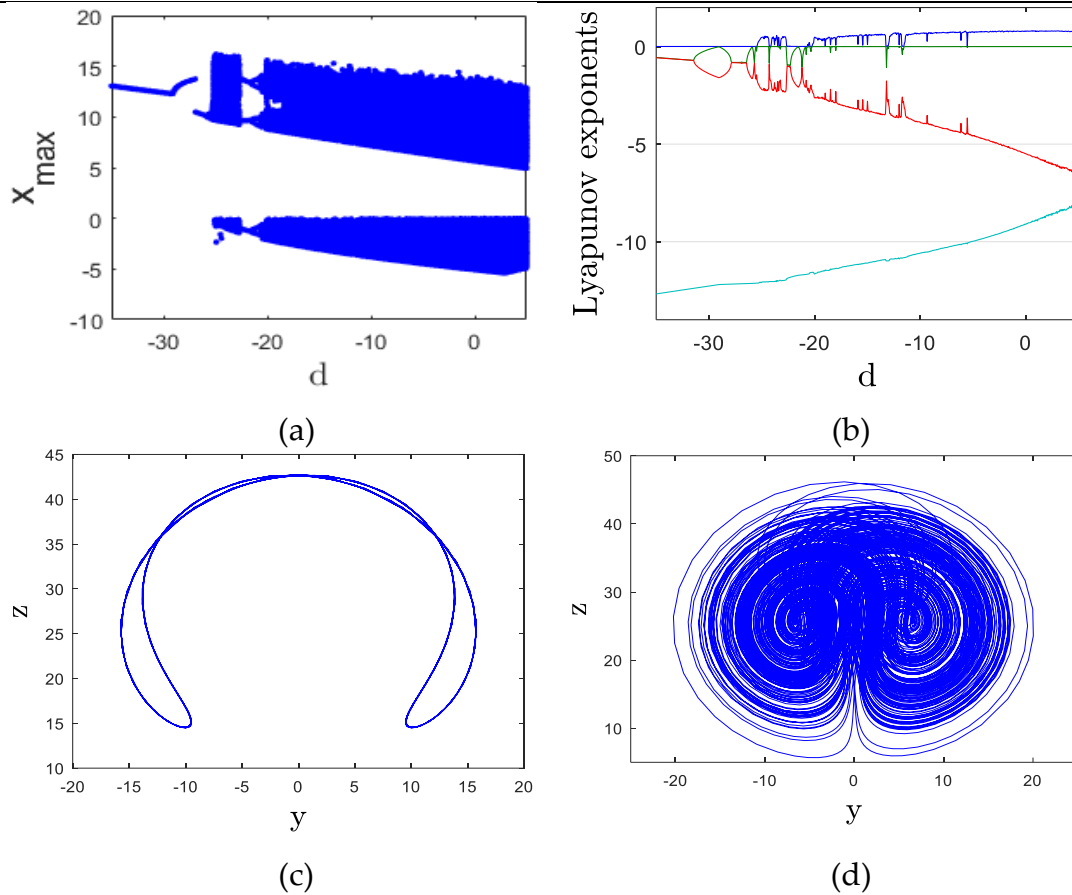


Figure 5. Chaotic exhibition of system (4): (a) bifurcation diagram, (b) Lyapunov exponents, (c) y-z periodic attractor for $d=-27$, (d) y-z chaotic attractor for $d=1$.

Within the range of d ($[-25.5, -22.8]$, $[-20.2, 5]$), System (5) predominantly displays chaotic behavior. However, exceptions occur at specific values such as $d = [(-24.3, -24.15), (-23.35, -23.25), (-13.25, -13), (-11.75, -11.55)]$, $d = -18.5$, and $d = -18$, where periodic behavior is observed, as depicted in Figure 5(a). Additionally, Figure 5(b) highlights a positive Maximum Lyapunov Exponent (MLE) within this range. To provide further insight, we present a visualization of the chaotic attractor in Figure 5(d) corresponding to the case when $d = 1$. The resulting Lyapunov Exponents according to this setting are: $LE1 = 0.772$, $LE2 = 0$, $LE3 = -5.669$, and $LE4 = -8.903$.

Contingency reserves in supply chain management refer to the additional inventory or resources kept to buffer against uncertainties and disruptions [36]. Chaotic behavior due to poorly managed contingency reserves is characterized by erratic and unpredictable fluctuations in inventory levels, leading to inefficiencies and instability in the supply chain. In the chaotic regime, phase portraits of supply chain variables (e.g., inventory level vs. order quantity) show intricate, non-repeating patterns, indicating high sensitivity to initial conditions. Periodic behavior, in contrast, is characterized by regular, repeating patterns in the supply chain dynamics due to well-managed contingency reserves. This occurs when contingency reserves are appropriately sized and consistently utilized to buffer against demand variability and disruptions.

1.3.5. Influence of parameter "p" on system's behavior

In this subsection, we explore the impact of parameter 'p' on the system's behavior by systematically varying it within the range of [0.5, 10]. This observation was drawn from the dynamics of the bifurcation diagram and Lyapunov exponents spectrum.

When choosing p between ([0.5, 9.3]), we observe a clear sign of chaotic behavior in System (4), as found in Figure 6(a). Furthermore, Figure 6(b) indicates a positive Maximum Lyapunov Exponent (MLE) within this range. To provide a deeper understanding, we present a visualization of the chaotic attractor in Figure 6(c) corresponding to the scenario when p = 3. The resulting Lyapunov Exponents according to this setting are: LE1 = 1.022, LE2 = 0, LE3 = -5.601, and LE4 = -9.222.

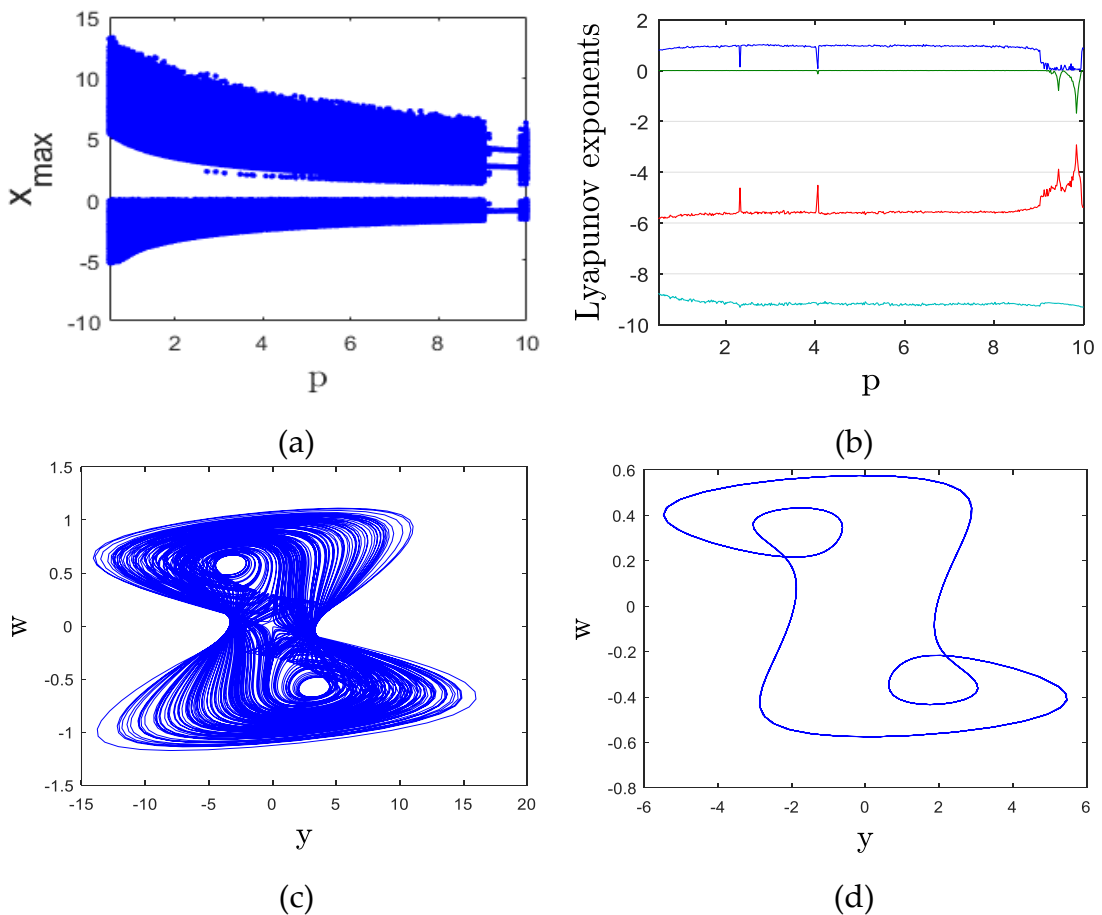
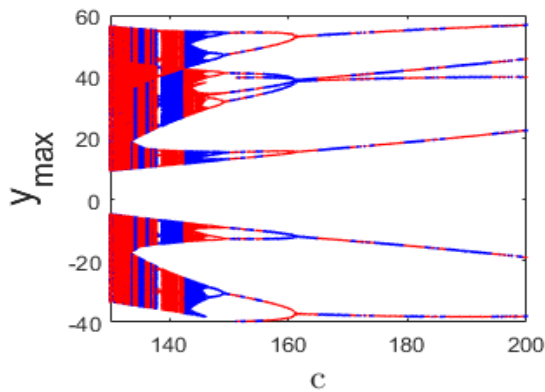


Figure 6. Chaotic exhibition of system (4): (a) bifurcation diagram, (b) Lyapunov exponents, (c) y - w chaotic attractor for $p=3$, (d) y - w periodic attractor for $p=9.8$

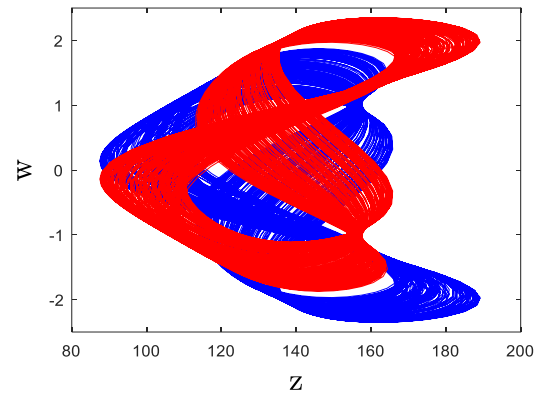
For the range of p [9.3, 10], System (4) demonstrates periodic behavior, except for instances when p is in the intervals [9.94, 10], $p = 9.35$, and $p = 9.5$, as illustrated in Figure 6(a). Notably, Figure 6(b) reveals that the MLE is zero within this interval. Figure 6(d) illustrates the periodic attractor for the scenario when $p = 9.8$. The

resulting Lyapunov Exponents according to this setting are: $LE1 = 0$, $LE2 = -0.777$, $LE3 = -3.791$, and $LE4 = -9.238$.

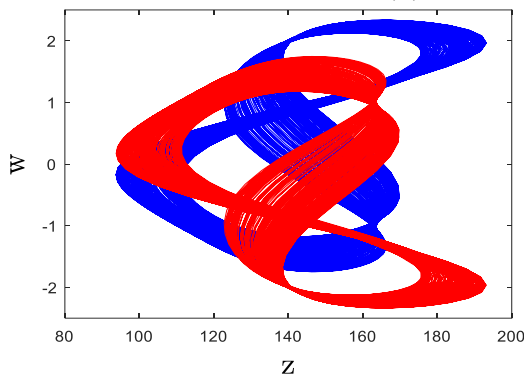
Chaotic behavior due to improperly managed safety stock is characterized by irregular and unpredictable fluctuations in inventory levels, leading to instability in the supply chain [37]. Factors contributing to chaotic behavior include inappropriate sizing of safety stock and inconsistent replenishment policies. Chaotic behavior due to safety stock can lead to frequent overstocking or stockouts, increasing holding costs and reducing service levels. Also, periodic behavior allows for consistent service levels and efficient inventory management, reducing the likelihood of stockouts and excess inventory.



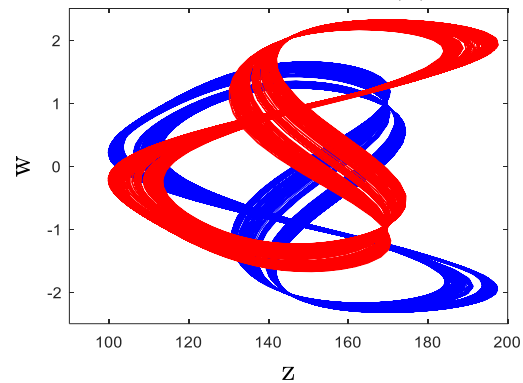
(a)



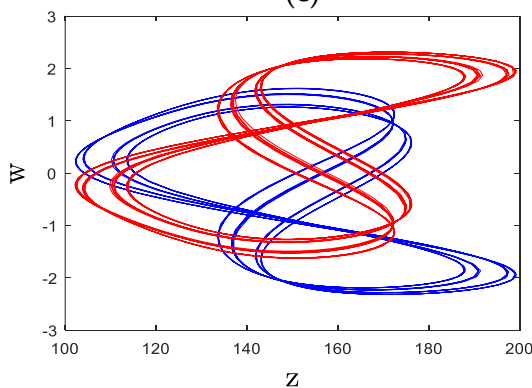
(b)



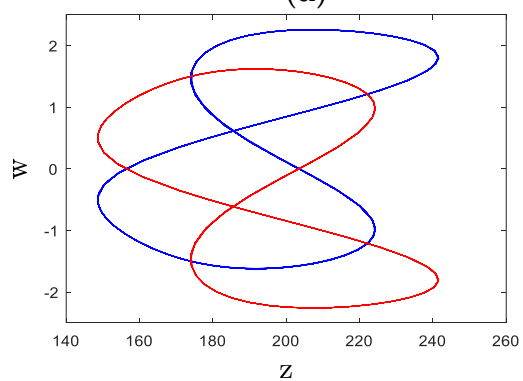
(c)



(d)



(e)



(f)

Figure 7. Chaotic exhibition of system (4): (a) bifurcation diagram, (b) two coexisting chaotic attractors for $c=135$, (c) two coexisting chaotic attractors for $c=140$, (d) two coexisting chaotic attractors for $c=145$, (e) two coexisting periodic attractors for $c=147$, (f) two coexisting periodic attractors for $c=190$.

1.3.6. Influence of initial conditions on system's behavior

In this section, we explore how the choice of initial conditions potentially affects the behavior of the system we have proposed. We discuss its multistability and the coexistence of different chaotic attractors by considering a fixed parameter values yet with different initial points [38-41]. To demonstrate this interesting phenomenon, we choose two distinct initial points: $[0.04 \ 0.04 \ 0.04 \ 0.04]$, shown in blue, and $[-0.04 \ 0.04 \ 0.04 \ 0.04]$, shown in red. Next, we create a bifurcation diagram for System (4) with c values ranging from 130 to 200. The resulting diagram, displayed in Figure 7(a), clearly shows the presence of multistability in the system.

In Figures 7(b), 7(c), and 7(d), you can see three pairs of coexisting chaotic attractors generated by system (4) for $c=135$, $c=140$, and $c=145$, respectively. Figures 7(e) and 7(f) depicts two pairs of coexisting periodic attractors for $c=147$ and $c=190$, respectively. The existence of coexisting distinct attractors under identical parameter settings underscores the complex dynamical nature of the proposed system, offering valuable insights into its behavior and potential applications.

1.4 Sliding Mode Controller

Traditionally, two main steps are considered in the design of sliding model control. The first step is the selection of the sliding surface and the second step is the control law to stay on the sliding surface [42,43]. In practice and computer implementations, other steps must be considered. Therefore, in this article, all the steps of designing the sliding model controller will be described. Initially, with initial conditions the system will have an output. This output will be compared with the desired values and the error will be obtained. The error block has two outputs, the first is the error and the second is its derivative.

In the next block, the sliding method calculates the sliding surface and its derivative using the error and the derivative of the error (of course, the sliding surface is selected by the designer, but finally the slip surface and the derivative of the sliding surface must be calculated). The equivalent control law is obtained from the two parameters of the sliding surface and the derivative of the sliding surface. This control law is called equivalent controller. In the design of the sliding mode controller, the exponential reaching law is added to the equivalent controller. Finally, the sliding model controller will be activated. This cycle continues until the output of the system tends to the desired values. The block diagram in Figure 8 depicts this cycle.

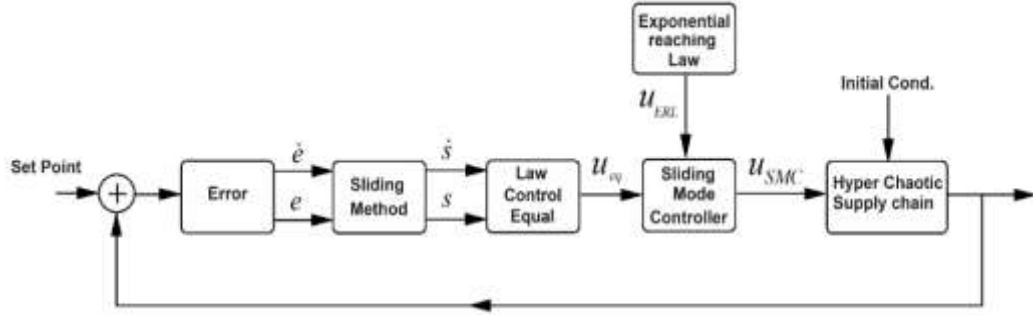


Figure 8. Block diagram of the design steps of the sliding model controller
In this paper, the main goal is to eliminate the chaotic behavior in the 4D chaotic supply chain.

So, equations (6) are rewritten as follows:

$$\begin{cases} \dot{x} = a(y - x) + dw + u_{SMC_x} \\ \dot{y} = cx - xz - y + u_{SMC_y} \\ \dot{z} = xy - bz + px^2 + u_{SMC_z} \\ \dot{w} = -x - aw + u_{SMC_w} \end{cases} \quad (6)$$

that $u_{SMC_x}, u_{SMC_y}, u_{SMC_z}, u_{SMC_w}$ are the proposed sliding model controllers and should be designed.

Step 1: The first step is to calculate the error. The error function is defined as follows:

$$\begin{cases} e_x = x - x^* \\ e_y = y - y^* \\ e_z = z - z^* \\ e_w = w - w^* \end{cases} \quad (7)$$

where x^*, y^*, z^*, w^* are the desired values (set point) to reach our control goal.

Step 2: Calculation of the error derivative, according to equation (7), so:

$$\begin{cases} \dot{e}_x = \dot{x} - \dot{x}^* \\ \dot{e}_y = \dot{y} - \dot{y}^* \\ \dot{e}_z = \dot{z} - \dot{z}^* \\ \dot{e}_w = \dot{w} - \dot{w}^* \end{cases} \quad (8)$$

Step 3: The selection of the sliding surface is very important in the design problem of the sliding model controller. Therefore, the sliding surface in this design is considered as follows:

$$\begin{cases} s_x = e_x(t) + \int_0^t \zeta_x e_x(\tau) d\tau \\ s_y = e_y(t) + \int_0^t \zeta_y e_y(\tau) d\tau \\ s_z = e_z(t) + \int_0^t \zeta_z e_z(\tau) d\tau \\ s_w = e_w(t) + \int_0^t \zeta_w e_w(\tau) d\tau \end{cases} \quad (9)$$

where $\zeta_x, \zeta_y, \zeta_z, \zeta_w$ are constant values.

Step 4: To determine the derivative of the sliding surface, the derivative is taken from equation (9):

$$\begin{cases} \dot{s}_x = \dot{e}_x(t) + \zeta_x e_x(t) \\ \dot{s}_y = \dot{e}_y(t) + \zeta_y e_y(t) \\ \dot{s}_z = \dot{e}_z(t) + \zeta_z e_z(t) \\ \dot{s}_w = \dot{e}_w(t) + \zeta_w e_w(t) \end{cases} \quad (10)$$

To reach the equivalent control law, the condition $s=0$ must be satisfied. Therefore:

$$\begin{cases} \dot{e}_x(t) + \zeta_x e_x(t) = 0 \\ \dot{e}_y(t) + \zeta_y e_y(t) = 0 \\ \dot{e}_z(t) + \zeta_z e_z(t) = 0 \\ \dot{e}_w(t) + \zeta_w e_w(t) = 0 \end{cases} \quad (11)$$

Step 5: Determine the equivalent controller. By replacing equation (8) in equation (11) and simplifying, the equivalent controller is obtained:

$$\begin{cases} u_{x_{eq}} = -a(y-x) - dw - x^* - \zeta_x e_x(t) \\ u_{y_{eq}} = -cx + xz + y - y^* - \zeta_y e_y(t) \\ u_{z_{eq}} = -xy + bz - px^2 - z^* - \zeta_z e_z(t) \\ u_{w_{eq}} = x + aw - w^* - \zeta_w e_w(t) \end{cases} \quad (12)$$

where u are equivalent controllers. To achieve the final model sliding control, the exponential control law should also be added to the equivalent controller. So:

$$\begin{cases} u_{SMC_x} = u_{x_{eq}} + u_{x_{ERL}} \\ u_{SMC_y} = u_{y_{eq}} + u_{y_{ERL}} \\ u_{SMC_z} = u_{z_{eq}} + u_{z_{ERL}} \\ u_{SMC_w} = u_{w_{eq}} + u_{w_{ERL}} \end{cases} \quad (13)$$

Step 6: Obtaining the exponential control law, which is the exponential control law in equation (13) and is obtained from the following relationship.

$$\begin{cases} u_{x_{ERL}} = k_x s_x + \alpha_x \frac{s_x}{|s_x| + \varepsilon_x} \\ u_{y_{ERL}} = k_y s_y + \alpha_y \frac{s_y}{|s_y| + \varepsilon_y} \\ u_{z_{ERL}} = k_z s_z + \alpha_z \frac{s_z}{|s_z| + \varepsilon_z} \\ u_{w_{ERL}} = k_w s_w + \alpha_w \frac{s_w}{|s_w| + \varepsilon_w} \end{cases} \quad (14)$$

In the last equation, k, ε are the gains of the exponential control law. Of course, it is obvious that:

$$\lim_{\varepsilon \rightarrow 0} \left(\alpha \frac{s}{|s| + \varepsilon} \right) = \alpha \operatorname{sign}(s) \quad (15)$$

Verification of the sliding model controller design is done with the help of Theorem 1.

Theorem 1: The behavior of the chaotic equations of the supply chain (6) under the controller of the following proposed sliding model tends to the desired values when the values initial condition $x(0), y(0), z(0), w(0) \in \mathbb{R}$.

$$\begin{cases} u_{SMC_x} = -a(y-x) - dw - x^* - \zeta_x e_x(t) + k_x s_x + \alpha_x \frac{s_x}{|s_x| + \varepsilon_x} \\ u_{SMC_y} = -cx + xz + y - y^* - \zeta_y e_y(t) + k_y s_y + \alpha_y \frac{s_y}{|s_y| + \varepsilon_y} \\ u_{SMC_z} = -xy + bz - px^2 - z^* - \zeta_z e_z(t) + k_z s_z + \alpha_z \frac{s_z}{|s_z| + \varepsilon_z} \\ u_{SMC_w} = x + aw - w^* - \zeta_w e_w(t) + k_w s_w + \alpha_w \frac{s_w}{|s_w| + \varepsilon_w} \end{cases} \quad (16)$$

Proof 1: Consider the candidate Lyapunov function as follows:

$$V(s) = \frac{1}{2} (s_x^2 + s_y^2 + s_z^2 + s_w^2) \quad (17)$$

If the equation (17) is derived, then:

$$\dot{V}(s) = \dot{s}_x s_x + \dot{s}_y s_y + \dot{s}_z s_z + \dot{s}_w s_w \quad (18)$$

By inserting and simplifying equation (18):

$$\begin{aligned}
\dot{V}(s) &= s_x(\dot{e}_x(t) + \zeta_x e_x(t)) + s_y(\dot{e}_y(t) + \zeta_y e_y(t)) + \\
&\quad s_z(\dot{e}_y(t) + \zeta_y e_y(t)) + s_w(\dot{e}_w(t) + \zeta_w e_w(t)) \quad (19) \\
&\Rightarrow s_x(k_x s_x + \alpha_x \frac{s_x}{|s_x| + \varepsilon_x}) + s_y(k_y s_y + \alpha_y \frac{s_y}{|s_y| + \varepsilon_y}) + \\
&\quad s_z(k_z s_z + \alpha_z \frac{s_z}{|s_z| + \varepsilon_z}) + s_w(k_w s_w + \alpha_w \frac{s_w}{|s_w| + \varepsilon_w})
\end{aligned}$$

Equation (19) will always be negative ($\dot{V}(s) < 0$) if and only if $\alpha_{x,y,z,w}, k_{x,y,z,w} < 0$

In the numerical simulation, MATLAB software is used to calculate the supply chain responses of equation (6). The initial condition values are equal to $[x(0) \ y(0) \ z(0) \ w(0)]^T = [0.04 \ 0.04 \ 0.04 \ 0.04]$. The sliding mode controller parameters are equal to $\alpha_{x,y,z,w} = 0.01, k_{x,y,z,w} = -0.1$ and $\zeta_{x,y,z,w} = -2$ are also selected. The desired values in this part of the simulation are zero ($x^* = y^* = z^* = w^* = 0$). Figure 9 shows the new 4D chaotic supply chain under the proposed sliding model controller. The control strategy is activated from time $t=4$.

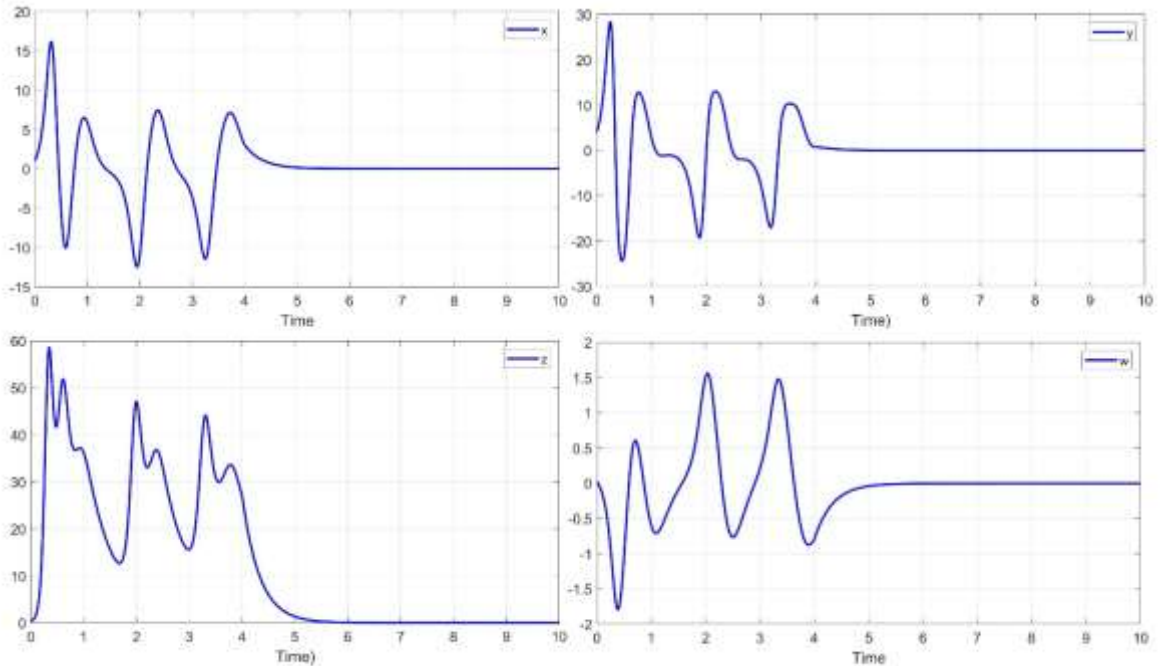


Figure 9. Elimination of chaotic behavior in 4D supply chain with the proposed sliding model control method

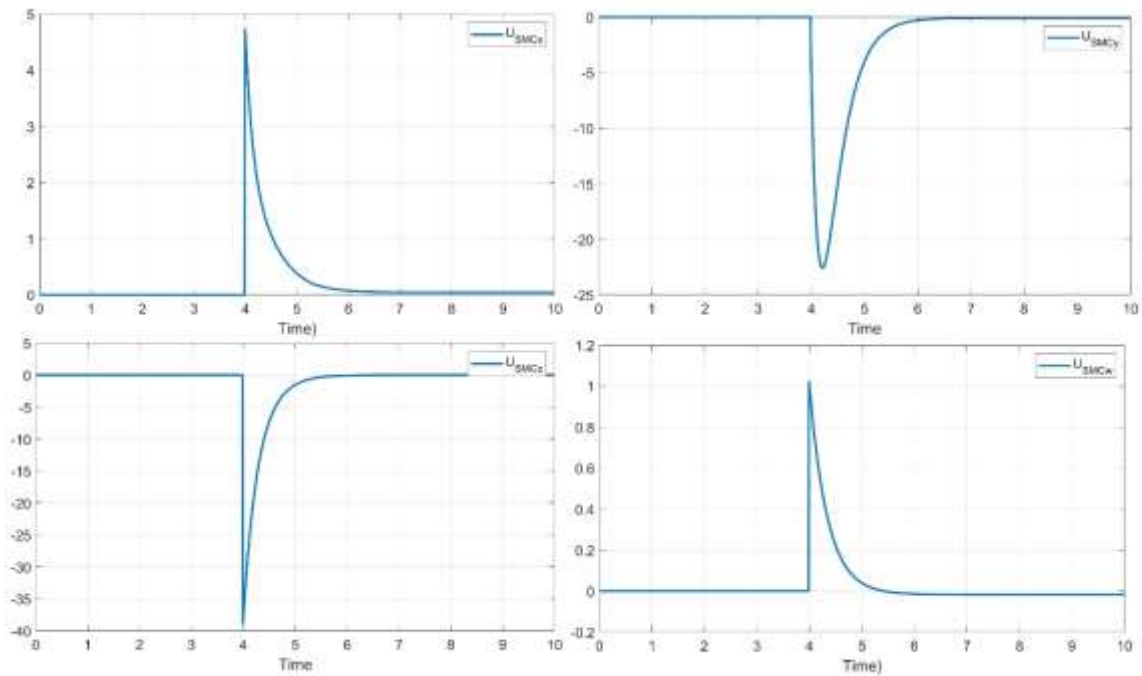


Figure 10. Behavior of the proposed sliding model controller

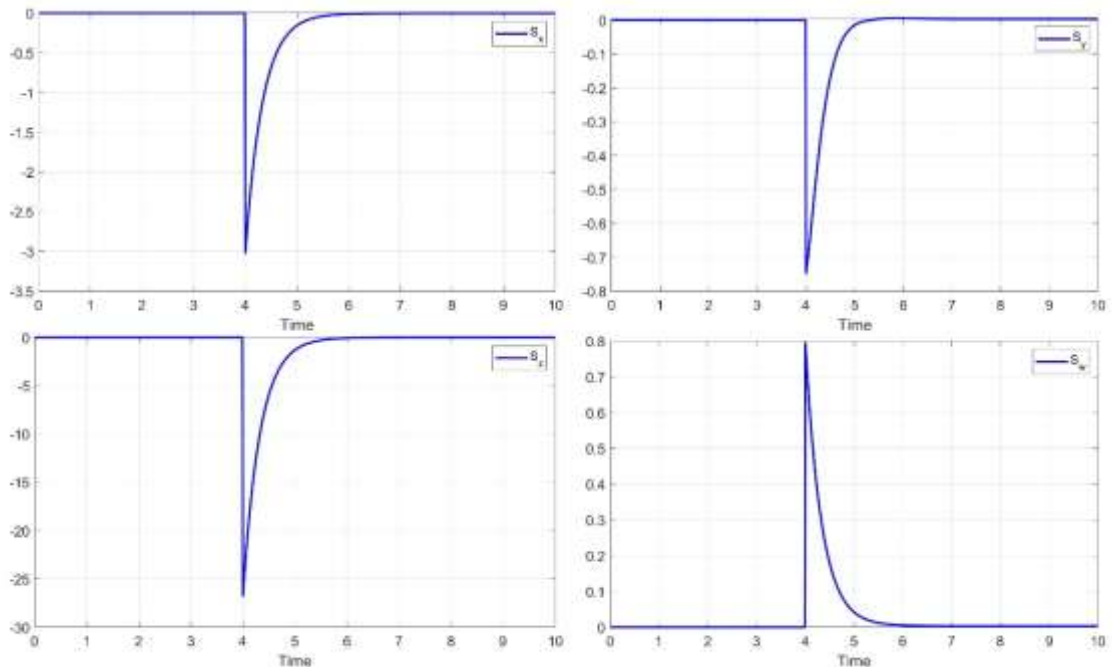


Figure 11. The behavior of the sliding surface

Figure 10 depicts the behavior of the proposed sliding model controller. As can be seen from Figure 10, the controller has reached zero value after a short time. Figure 11 shows that the sliding surface has converged to zero exponentially over time.

In the other part of the simulation, the tracking of other desired values is investigated. In this way, after reaching the first desired values, the second desired values are tracked.

Table 1. shows the different time sequences.

Seq.	Time	Desire value	Sliding mode
1	$0 < \text{Time} < 4$	none	off
2	$4 < \text{Time} < 10$	$x^* = y^* = z^* = w^* = 0$	on
3	$10 < \text{Time} < \infty$	$x^* = y^* = z^* = w^* = 5$	on

When physical systems are involved in chaos, they cause great damage to organizations and systems in the real world. Therefore, controller design methods should be able to remove chaotic behavior from the system in a short period of time and also track it if desired values are required. Therefore, the time to reach stability is defined from the time the controller is applied until the zero error is reached. In the sliding model controller design method, the time to reach stability and eliminate chaos is approximately equal to $t=1.8$. This value can be controlled by setting the parameters $\zeta_x, \zeta_y, \zeta_z, \zeta_w$ in equation (9). Figure 14 shows the comparison of chaotic supply chain behavior with changing values $\zeta_x, \zeta_y, \zeta_z, \zeta_w$, and Figure 15 shows the behavior of the proposed sliding model controller with different $\zeta_x, \zeta_y, \zeta_z, \zeta_w$ values.

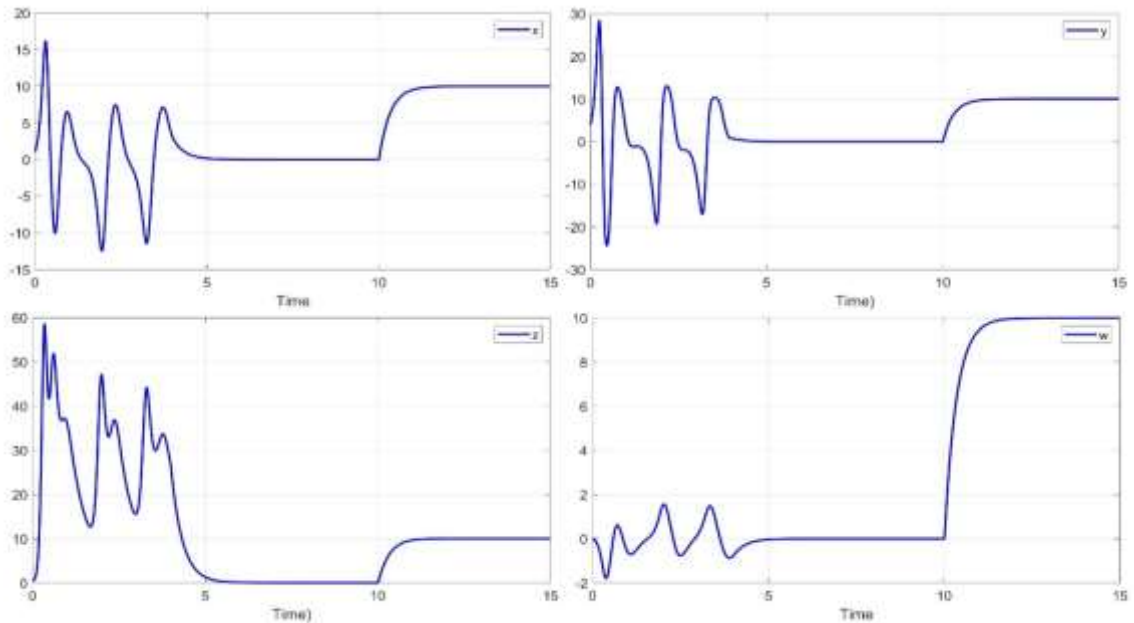


Figure 12. Chaos removal and optimal value tracking under the proposed sliding model controller

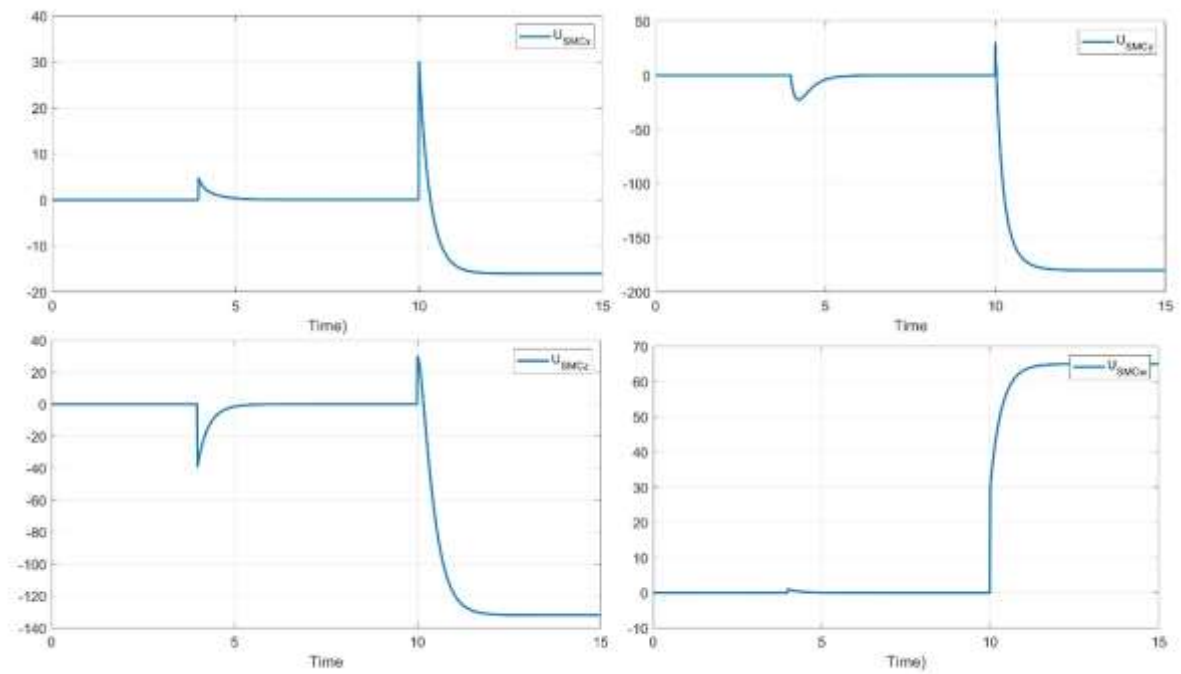


Figure 13. The behavior of the sliding model controller in order to track the desire values after removing the chaos

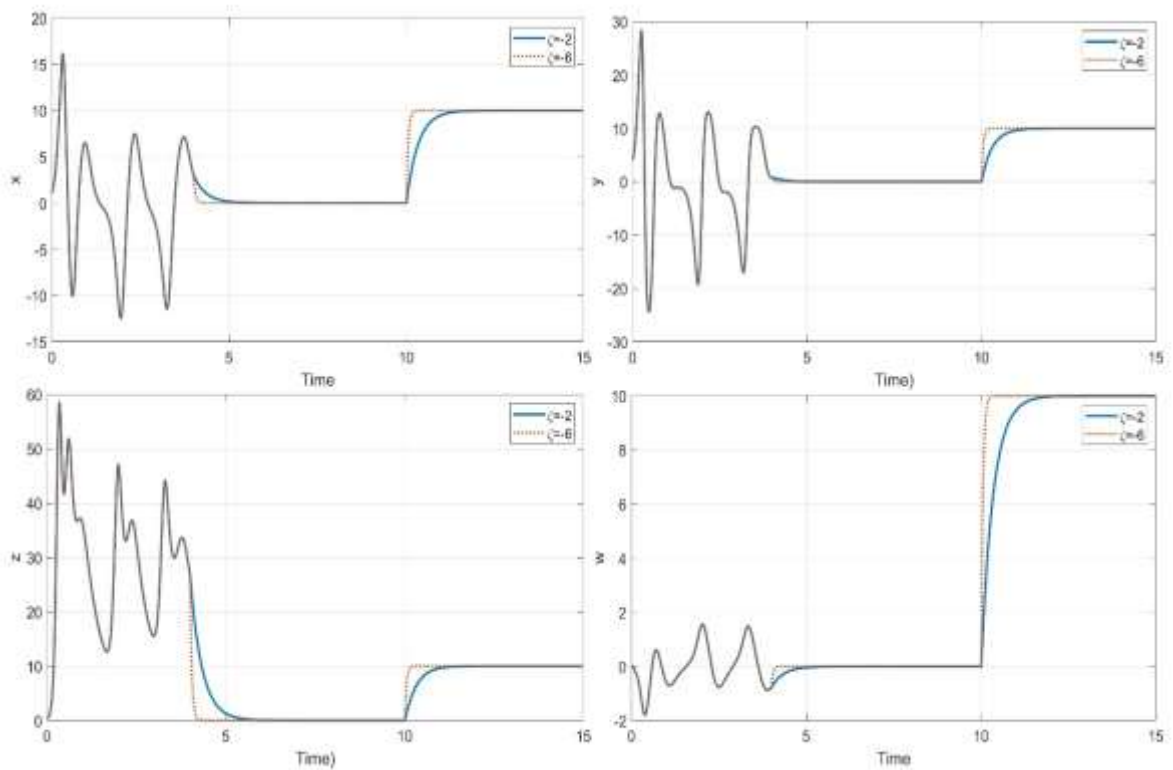


Figure 14. Chaotic supply chain behavior with changing values $\zeta_x, \zeta_y, \zeta_z, \zeta_w$

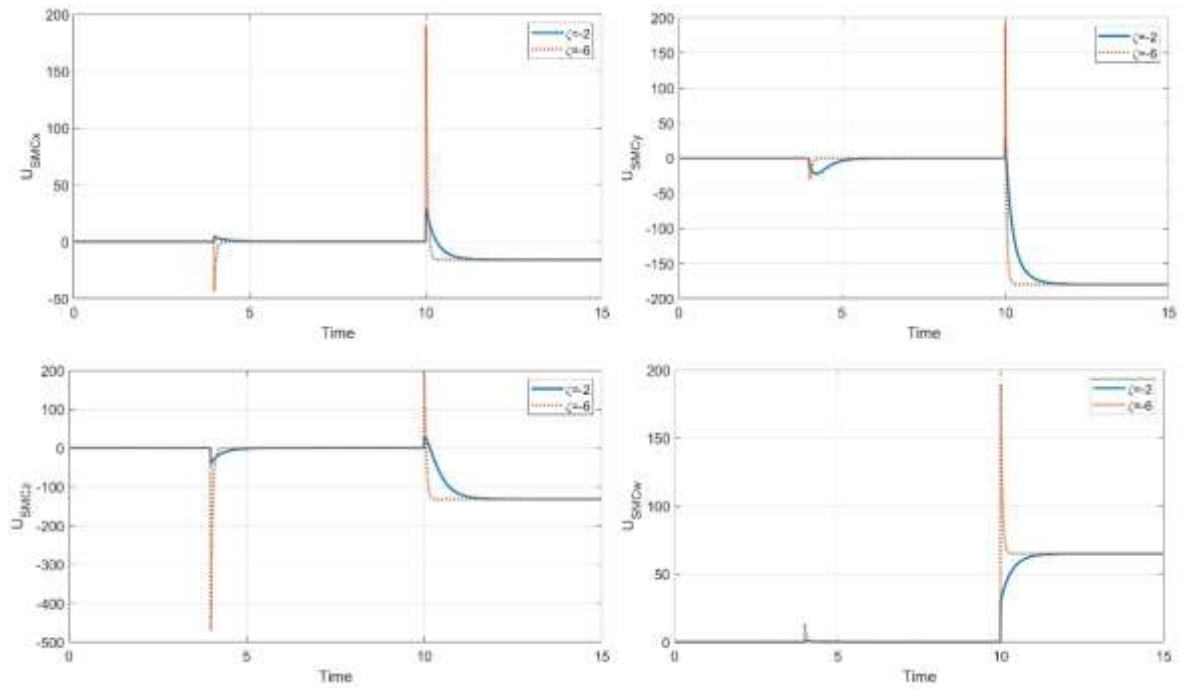


Figure 15. The behavior of the sliding model controller for remove chaotic supply chain behavior with changing values $\zeta_x, \zeta_y, \zeta_z, \zeta_w$

As can be seen, the more negative zeta values increase the speed of convergence towards the desired values. But the important point is the controller's behavioral conditions, which have sharp points and more magnitude. Controller behavior can represent real-world implementation cost. In other words, in physical systems, the control signal is applied to the actuator, but if this signal has high frequencies, the actuator may not be able to respond to it. In supply chain systems, the control signal is the same as management decisions. Also, the actuator in supply chain systems is interpreted as organizational agility. Therefore, if an organization is agile and fast, it can respond to quick management decisions. Otherwise, in physical systems or supply chain systems, the fast behavior of the controller is not seen by the driver.

1.5 Conclusion

This paper delves into the intricate dynamics of supply chains, highlighting the challenges posed by their interconnected components and susceptibility to disruptions. Our research utilizes dynamical and multistability analyses to explore nonlinear behaviors and identify potential risks within these systems. Key findings from our dynamical analysis demonstrated how transport risk, quality risk, distortion, contingency reserves, and safety stock impact supply chain management. Each of these factors was shown to influence the stability and efficiency of supply chain operations significantly. Moreover, we introduced a sliding method for computing the sliding surface and its derivative, along with the derivation of an equivalent control law. This method presents promising avenues for controlling supply chain dynamics by providing a robust mechanism to manage the complexities and nonlinearities inherent in supply chains. Our sliding mode controller was

validated through simulations, which underscored its effectiveness in stabilizing supply chain operations and enhancing performance. In practical terms, this controller can be implemented in supply chain management software and systems to automatically adjust key parameters such as order quantities, inventory levels, and safety stock in response to real-time data. Due to computational limitations, real applications will be implemented for future research.

1.6 References

1. Bidhandi, H. M.; Yusuff, R. M.; Ahmad, M. M. H. M.; Bakar, M. R. A. Development of a new approach for deterministic supply chain network design. *European Journal of Operational Research*, **2009**, 198(1), 121-128.
2. Biswas, P.; Kumar, S.; Jain, V.; Chandra, C. Measuring supply chain reconfigurability using integrated and deterministic assessment models. *Journal of Manufacturing Systems*, **2019**, 52, 172-183.
3. Göksu, A.; Kocamaz, U. E.; Uyaroğlu, Y. Synchronization and control of chaos in supply chain management. *Computers & Industrial Engineering*, **2015**, 86, 107-115.
4. Stapleton, D.; Hanna, J. B.; Ross, J. R. Enhancing supply chain solutions with the application of chaos theory. *Supply Chain Management: An International Journal*, **2006**, 11(2), 108-114.
5. Wang, J.; Chi, D.; Wu, J.; Lu, H. Y. Chaotic time series method combined with particle swarm optimization and trend adjustment for electricity demand forecasting. *Expert Systems with Applications*, **2011**, 38(7), 8419-8429.
6. Yuan, X. Understanding complex dynamics in inventory management with endogenous demand under social interactions: a chaos perspective. *International Journal of Systems Science: Operations & Logistics*, **2023**, 10(1), 2225715.
7. Chryssolouris, G.; Giannelos, N.; Papakostas, N.; Mourtzis, D. Chaos theory in production scheduling. *CIRP Annals*, **2004**, 53(1), 381-383.
8. Lu, J. C.; Nie, X. Y. (2019, February). Logistics distribution path optimization research based on adaptive chaotic disturbance flies optimization algorithm. In *IOP Conference Series: Earth and Environmental Science*, **2019**, (Vol. 237, No. 5, p. 052068). IOP Publishing.
9. Norouzi Nav, H.; Jahed Motlagh, M. R. Makui, A. Robust controlling of chaotic behavior in supply chain networks. *Journal of the Operational Research Society*, **2017**, 68, 711-724.
10. Ma, J.; Ren, H.; Yu, M.; Zhu, M. Research on the complexity and chaos control about a closed-loop supply chain with dual-channel recycling and uncertain consumer perception. *Complexity*, **2018**, 2018(9), 1-13.
11. Guo, Y.; Ma, J. Research on game model and complexity of retailer collecting and selling in closed-loop supply chain. *Applied Mathematical Modelling*, **2013**, 37(7), 5047-5058.
12. Açıkgöz, N.; Çağıl, G.; Uyaroğlu, Y. The experimental analysis on safety stock effect of chaotic supply chain attractor. *Computers & Industrial Engineering*, **2020**, 150, 106881.
13. Hwarng, H. B.; Xie, N. Understanding supply chain dynamics: A chaos perspective. *European Journal of Operational Research*, **2008**, 184(3), 1163-1178.
14. Anne, K. R.; Chedjou, J. C.; Kyamakya, K. Bifurcation analysis and synchronization issues in a three-echelon supply chain. *International Journal of Logistics: Research and Applications*, **2009**, 12(5), 347-362.
15. Mondal, S. A new supply chain model and its synchronization behaviour. *Chaos, Solitons & Fractals*, **2019**, 123, 140-148.

16. Tirandaz, H. Complete synchronisation of supply chain system using adaptive integral sliding mode control method. *International Journal of Modelling, Identification and Control*, **2019**, 31(4), 314-322.
17. Luo, Y.; Deng, F.; Ling, Z.; Cheng, Z. Local H^∞ synchronization of uncertain complex networks via non-fragile state feedback control. *Mathematics and Computers in Simulation*, **2019**, 155, 335-346.
18. Xu, X.; Lee, S. D.; Kim, H. S.; You, S. S. Management and optimisation of chaotic supply chain system using adaptive sliding mode control algorithm. *International journal of production research*, **2021**, 59(9), 2571-2587.
19. Kocamaz, U. E.; Taşkın, H.; Uyaroğlu, Y.; Göksu, A. Control and synchronization of chaotic supply chains using intelligent approaches. *Computers & Industrial Engineering*, **2016**, 102, 476-487.
20. Hamidzadeh, S. M.; Rezaei, M.; Ranjbar-Bourani, M. Chaos synchronization for a class of uncertain chaotic supply chain and its control by ANFIS. *International Journal of Production Management and Engineering*, **2023**, 11(2), 113-126.
21. Nav, H. N.; Jahedmotlagh, M. R.; Makui, A. Robust H^∞ control for chaotic supply chain networks. *Turkish Journal of Electrical Engineering and Computer Sciences*, **2017**, 25(5), 3623-3636.
22. Liu, Z.; Jahanshahi, H.; Volos, C.; Bekiros, S.; He, S.; Alassafi, M. O.; Ahmad, A. M. Distributed consensus tracking control of chaotic multi-agent supply chain network: A new fault-tolerant, finite-time, and chatter-free approach. *Entropy*, **2021**, 24(1), 33.
23. Shi, L.; Guo, W.; Wang, L.; Bekiros, S.; Alsubaie, H.; Alotaibi, A.; Jahanshahi, H. Stochastic Fixed-Time Tracking Control for the Chaotic Multi-Agent-Based Supply Chain Networks with Nonlinear Communication. *Electronics*, **2022**, 12(1), 83.
24. Yan-Chen, W.; De-Gang, Z.; Xu, W. Prediction model of supply chain demand based on fuzzy neural network with chaotic time series. In *Proceedings of 2013 IEEE International Conference on Service Operations and Logistics, and Informatics*, 2013, (pp. 450-455). IEEE.
25. Ngoc Cuong, T.; Xu, X.; Lee, S. D.; You, S. S. Dynamic analysis and management optimization for maritime supply chains using nonlinear control theory. *Journal of International Maritime Safety, Environmental Affairs, and Shipping*, **2020**, 4(2), 48-55.
26. Sepestanaki, M. A.; Rezaee, H.; Soofi, M.; Fayazi, H.; Rouhani, S. H.; Mobayen, S. Adaptive continuous barrier function-based super-twisting global sliding mode stabilizer for chaotic supply chain systems. *Chaos, Solitons & Fractals*, **2024**, 182, 114828.
27. Hamidzadeh, S. M.; Rezaei, M.; Ranjbar-Buorani, M. Control and Synchronization of The Hyperchaotic Closedloop Supply Chain Network by PI Sliding Mode Control. *International Journal of Industrial Engineering & Production Research*, **2022**, 33(4), 1-13.
28. Johansyah, M. D.; Sambas, A.; Mobayen, S.; Vaseghi, B.; Al-Azzawi, S. F.; Sukono,; Sulaiman, I. M. Dynamical analysis and adaptive finite-time sliding mode control approach of the financial fractional-order chaotic system. *Mathematics*, **2022**, 11(1), 100.

-
29. Ramírez, S. A., Peña, G. Analysis of chaotic behaviour in supply chain variables. *Journal of Economics, Finance & Administrative Science*, **2011**, 16(31), 85.
 30. Ma, J.; Xie, L. The impact of loss sensitivity on a mobile phone supply chain system stability based on the chaos theory. *Communications in Nonlinear Science and Numerical Simulation*, **2018**, 55, 194-205.
 31. Cuong, T. N.; Kim, H. S.; You, S. S. Decision support system for managing multi-echelon supply chain networks against disruptions using adaptive fractional order control algorithm. *RAIRO-Operations Research*, **2023**, 57(2), 787-815.
 32. Pellegrino, R.; Costantino, N.; Tauro, D. The value of flexibility in mitigating supply chain transportation risks. *International Journal of Production Research*, **2021**, 59(20), 6252-6269.
 33. Liu, C. H.; Xiong, W. Modelling and simulation of quality risk forecasting in a supply chain. *International Journal of Simulation Modelling*, **2015**, 2, 359-370.
 34. Ma, J.; Lou, W.; Tian, Y. Bullwhip effect and complexity analysis in a multi-channel supply chain considering price game with discount sensitivity. *International Journal of Production Research*, **2019**, 57(17), 5432-5452.
 35. Dominguez, R.; Cannella, S.; Framinan, J. M. The impact of the supply chain structure on bullwhip effect. *Applied Mathematical Modelling*, **2015**, 39(23-24), 7309-7325.
 36. Lücker, F.; Seifert, R. W.; Biçer, I. Roles of inventory and reserve capacity in mitigating supply chain disruption risk. *International Journal of Production Research*, **2019**, 57(4), 1238-1249.
 37. Wei, Y.; Wang, H.; Qi, C. The impact of stock-dependent demand on supply chain dynamics. *Applied Mathematical Modelling*, 2013, 37(18-19), 8348-8362.
 38. Al-Azzawi, S. F.; Al-Hayali, M. A. Multistability and hidden attractors in a novel simple 5D chaotic Sprott E system without equilibrium points. *Journal of Interdisciplinary Mathematics*, **2022**, 25(5), 1279-1294.
 39. Al-hayali, M. A.; Al-Azzawi, F. S. A 4D hyperchaotic Sprott S system with multistability and hidden attractors. In *Journal of Physics: Conference Series*, **2021**, (Vol. 1879, No. 3, p. 032031). IOP Publishing.
 40. Benkouider, K.; Vaidyanathan, S.; Sambas, A.; Tlelo-Cuautle, E.; Abd El-Latif, A. A.; Abd-El-Atty, B.; Kumam. A new 5-D multistable hyperchaotic system with three positive Lyapunov exponents: Bifurcation analysis, circuit design, FPGA realization and image encryption. *IEEE Access*, **2022**, 10, 90111-90132.
 41. Sambas, A.; Miroslav, M.; Vaidyanathan, S.; Ovilla-Martínez, B.; Tlelo-Cuautle, E.; Abd El-Latif, A. A.; Bonny, T. A New Hyperjerk System with a Half Line Equilibrium: Multistability, Period Doubling Reversals, Antimonotonicity, Electronic Circuit, FPGA Design and an Application to Image Encryption. *IEEE Access*, **2024**.
 42. Sambas, A.; Vaidyanathan, S.; Zhang, X.; Koyuncu, I.; Bonny, T.; Tuna, M.; Kumam, P.. A novel 3D chaotic system with line equilibrium: multistability, integral sliding mode control, electronic circuit, FPGA implementation and its image encryption. *IEEE Access*, **2022**, 10, 68057-68074.
 43. Cuong, T. N.; Kim, H. S.; Nguyen, D. A.; You, S. S. Nonlinear analysis and active management of production-distribution in nonlinear supply chain model using sliding mode control theory. *Applied Mathematical Modelling*, **2021**, 97, 418-437.

CHAPTER 2

Enhanced Chaotic Modeling of Supply Chains with

Market Shock and Intelligent Fuzzy Control

2.1 Introduction

The SCM plays a pivotal role in driving economic growth as it serves as the backbone of production, distribution, and consumption processes in both local and global markets [1]. A well-functioning supply chain ensures the efficient flow of goods, services, information, and capital across various sectors, enabling businesses to meet customer demands, minimize operational costs, and respond swiftly to market dynamics [2]. In the context of globalization, supply chains have become increasingly interconnected and complex, involving multiple stakeholders across borders, which amplifies their strategic importance in sustaining economic development [3]. However, the growth of the economy is often challenged by supply chain disruptions caused by factors such as natural disasters, geopolitical instability, pandemics, and sudden market shocks, which can lead to delays, shortages, and increased costs [4]-[6]. Additionally, uncertainties in demand forecasting, transportation bottlenecks, and quality control issues further exacerbate the fragility of modern supply chains [7]. These challenges not only affect individual businesses but also have cascading effects on national and global economies, highlighting the urgent need for more resilient, adaptive, and intelligent supply chain systems [8]. Therefore, enhancing supply chain performance through advanced modeling and robust control mechanisms is essential to ensure economic stability, competitiveness, and sustainable growth in an increasingly uncertain world [9]-[10].

Market shock is a critical factor to be studied in SCM because it represents sudden and often unpredictable changes in market conditions, such as abrupt fluctuations in demand, price volatility, supply disruptions, or external crises like pandemics and geopolitical conflicts [11]-[13]. These shocks can cause significant disturbances throughout the supply chain, leading to inventory imbalances, production delays, increased costs, and customer dissatisfaction [14]. Unlike gradual trends, market shocks can propagate rapidly and nonlinearly, making traditional supply chain models inadequate in capturing their true impact [15]. Studying market shocks allows researchers and practitioners to develop more robust and adaptive strategies that can anticipate, absorb, and recover from such disruptions [16]. By incorporating market shock dynamics into SCM, decision-makers can improve system resilience, optimize response strategies, and maintain continuity under volatile

conditions, which is essential for sustaining business operations and economic stability [17]-[20].

Chaos is important to study in SCM because it provides a powerful framework for understanding the complex, nonlinear, and sensitive behaviors that frequently arise in real-world logistics networks [21]-[22]. Unlike linear models, which assume predictable and proportional responses, chaotic models capture how small changes in input—such as delays, demand variations, or supplier disruptions—can lead to disproportionately large and unpredictable effects across the entire supply chain [23]. These dynamics are especially relevant in today's interconnected and rapidly changing markets, where feedback loops, lead times, and interdependencies often generate irregular patterns and instability [24]. By analyzing chaotic behavior, researchers and practitioners can identify early signs of disruption, understand the conditions under which instability emerges, and develop strategies to control or mitigate adverse outcomes [25]. Thus, chaos theory offers valuable insights into the hidden patterns and vulnerabilities within supply chains, enabling the design of more resilient, adaptive, and intelligent systems.

The application of Fuzzy Control (FC) in chaotic systems and SCM has gained increasing attention in recent literature due to its ability to handle uncertainty and the inherent complexity of such systems. Aslam et al. [26] implement a novel fuzzy control strategy for nonlinear SCM systems that explicitly accounts for the effects of lead times and enable smooth switching between multiple SCM sub-models by using the MRRG method. Liu et al. [27] develop a robust fuzzy adaptive control strategy for the synchronization of a newly proposed fractional-order three-echelon SCM exhibiting chaotic behavior and integrated to enhance performance and eliminate chattering effects using FC. Kocamaz et al. [28] implemented a hybrid intelligent control approach for managing chaos and achieving synchronization in SCM using ANN and ANFIS-based controllers. Cao et al. [29] developed a hybrid modeling and FC framework for SCM under disruption conditions using Petri nets and constructed a fuzzy-based operational model of SCM that integrates both continuous delivery rate dynamics and discrete disruption events. Xu et al. [30] improved the accuracy of SCM prediction and enhance system stability by developing a fuzzy neural network-based prediction and control model grounded in chaotic time series analysis. They reconstructed the sub-phase space using SCM time-series data, determine the saturated embedding dimension and the largest LE, and build a demand prediction model using FNN. Zhang et al. [31] develop a fuzzy robust control strategy for an uncertain closed-loop SCM that experiences time-varying delays in the remanufacturing process and transformed into a fuzzy dynamic model with time delay using the Takagi–Sugeno fuzzy modeling approach.

Despite the significant progress in the application of FC strategies across various supply chain contexts—ranging from handling lead times, synchronization of chaotic systems, integration with intelligent control methods, to managing disruptions and delays—there remains a lack of comprehensive studies that integrate chaotic modeling, multistability analysis, and FC in a high-dimensional nonlinear SCM subjected to external shocks such as market volatility. Most existing works focus on either control or prediction, but few address the combined challenges of chaotic dynamics, market-induced perturbations, and the need for adaptive, low-oscillation control within a unified framework. Therefore, this study fills a critical gap by proposing an enhanced N5DCSCM that incorporates market shock dynamics and is stabilized using an intelligent FC strategy, offering a novel approach to achieving robust and efficient control in complex and uncertain supply chain environments.

The main contribution and novelty of this work as follows:

- a. This study introduces an enhanced N5DCSCM by incorporating market shock dynamics, providing a more realistic representation of supply chain behavior under external uncertainties.
- b. The paper conducts an in-depth dynamic analysis of the proposed system dynamical analysis and multistability exploration. Additionally, amplitude control via rescaling and offset boosting techniques are applied to further enhance system controllability without eliminating chaotic characteristics.
- c. A fuzzy logic-based controller is designed to stabilize the proposed chaotic system, demonstrating its effectiveness in reducing system oscillations, ensuring smooth transitions between system states, and maintaining control even in the presence of unknown inputs.

2.2 Model of N5DCSCM

Cuong et al. [32] described a CSCM by the following 4-D system:

$$\begin{cases} \dot{R} = a(D - R) + dC \\ \dot{D} = cR - RM - D \\ \dot{M} = RD - bM \\ \dot{C} = -R - aC \end{cases} \quad (1)$$

Here, R denotes the product demand at the retailer, D represents the quantity supplied by the distributor, M refers to the amount produced by the manufacturer, and C signifies the product received by the customer. Additionally, the CSCM (1) incorporates several coefficients, including transport risk (a), quality risk (b), distortion (c), and contingency reserve (d). When $a = 2, b = 1.05, c = 26$

and $d = 1.5$, Cuong et al. (2023) witnessed a chaotic attractor exhibited by the CSCM (1) for the initial values $R(0) = D(0) = M(0) = C(0) = 0.04$. In fact, for $T = 1E4$ seconds, the LE for the CSCM (1) were found to be:

$$(2) \quad L_1 = 0.4228, \quad L_2 = 0, \quad L_3 = -2.9262, \quad L_4 = -3.5468$$

We have added market shock, the question is

$$(3) \quad \begin{cases} \dot{R} = a(D - R) + dC + \alpha S \\ \dot{D} = cR - RM - D \\ \dot{M} = RD - bM \\ \dot{C} = -R - \alpha C \\ \dot{S} = -R + \gamma S \end{cases}$$

In N5DCSCM (3), αS represent the direct effect of market shock on demand growth R and $\dot{S} = -R + \gamma S$ is shock dynamics depend on damping demand. In N5DCSCM (3), α is the sensitivity or amplification factor of external disturbances, γ is sensitivity of market shock to demand, and δ is the natural rate of shock reduction. The N5DCSCM (3) displays chaotic dynamics for the parameter values $(a, b, c, d, \alpha, \gamma, \delta) = (2, 1.05, 26, 1.5, 1, 2.8, 1)$. The LEs of the N5DCSCM (3) are calculated using numerical simulation with the initial condition $R(0) = D(0) = M(0) = C(0) = S(0) = 0.04$ as given below:

$$(LE_1, LE_2, LE_3, LE_4, LE_5) = (0.425546, 0, -2.3613, -2.3943, -4.5183)$$

The equilibrium of the N5DCSCM (3) can be found by solving the following system of equations.

$$2(D - R) + 1.5C + S = 0 \quad (4a)$$

$$26R - RM - D = 0 \quad (4b)$$

$$RD - 1.05M = 0 \quad (4c)$$

$$-R - 2C = 0 \quad (4d)$$

$$-2.8R + S = 0 \quad (4e)$$

From equations (4d) and (4e), we first determined the values of the variables C and S in terms of R . Specifically, solving equation (4d) yielded:

$$C = -\frac{R}{2} \quad (4f)$$

and solving equation (4e) gave:

$$S = \frac{R}{2.8} \quad (4g)$$

Next, we substituted these expressions for C and S into equation (4a). Upon simplification, this substitution led to the following expression for D :

$$D = 1.19643R \quad (4h)$$

We then substituted (4h) into equation (4b). Solving this equation resulted in a numerical value for M :

$$M = 24.80357$$

Now, using the values $D = 1.19643R$ and $M = 24.80357$, we substituted into equation (4c). Solving this equation yielded the final value of R :

$$R = 4.666$$

Finally, using $R = 4.666$, we substituted in to equations (4f), (4g) and (4h) and consequently determined the values

$$D = 5.582, C = -2.333, S = 1.666$$

Thus, the equilibrium point of the new system can be written as

$$E = (R, D, M, C, S) = (4.666, 5.582, 24.8036, -2.333, 1.666) \quad (5)$$

Now, the Jacobian matrix of the model (3) can be written as follows:

$$J = \begin{bmatrix} -a & a & 0 & d & \alpha \\ c-M & -1 & -R & 0 & -1 \\ D & R & -b & 0 & 0 \\ -1 & 0 & 0 & -a & 0 \\ -\gamma & 0 & 0 & 0 & \delta \end{bmatrix} \quad (6)$$

By substituting the values from equation (5) and parameters into the matrix (6), the Jacobian matrix (6) becomes as (7).

$$J(E) = \begin{bmatrix} -2 & 2 & 0 & 1.5 & 1 \\ 1.1964 & -1 & -4.666 & 0 & -1 \\ 5.582 & 4.666 & -1.05 & 0 & 0 \\ -1 & 0 & 0 & -2 & 0 \\ -2.8 & 0 & 0 & 0 & 1 \end{bmatrix} \quad (7)$$

The eigenvalues of the matrix (7) are

$$\begin{aligned}
\lambda_{1,2} &= -0.05576 \pm j4.98477 \\
\lambda_{3,4} &= -2.73131 \pm j0.938 \\
\lambda_5 &= 0.52414
\end{aligned} \tag{8}$$

The combination of negative and positive values in the eigenvalues (8) shows that the equilibrium point (E) of the N5DCSCM (3) is unstable saddle point. Figure 1 shows the chaotic attractors of the N5DCSCM (3) in various 2D planes.

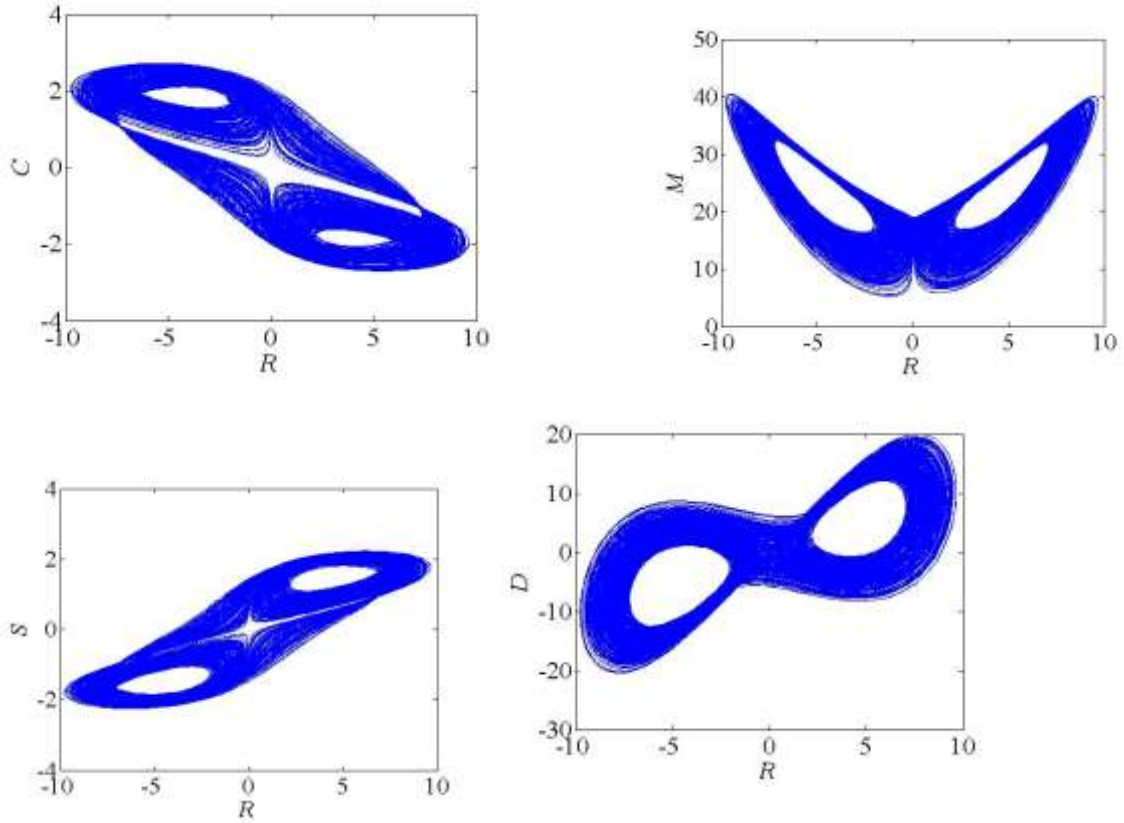


Figure 1. Chaotic attractors of the N5DCSCM (3) with the initial condition $R(0) = D(0) = M(0) = C(0) = S(0) = 0.04$.

2.3 Dynamic Analysis

In this section, the complex dynamics of the N5DCSCM (3) are examined using BD and LE spectra. The BD is a crucial tool in the analysis of chaotic models to understand how the system's behaviour changes a parameter is varied. It shows how a system transition from stable behaviour to chaos or vice versa as a parameter changes. The LE spectra play another central role in analysing and understanding chaotic systems. The most direct use of LE spectra is to quantify chaos. A positive LE indicates that nearby trajectories diverge exponentially, which is the defining characteristic of chaotic behaviour. In this work, the BD and LE spectra are plotted

with the initial conditions (0.04, 0.04, 0.04, 0.04, 0.04). The variation of the LE values is depicted in LE spectra, with LE_1 shown in blue, LE_2 in red, LE_3 in green, LE_4 in black, and LE_5 in magenta.

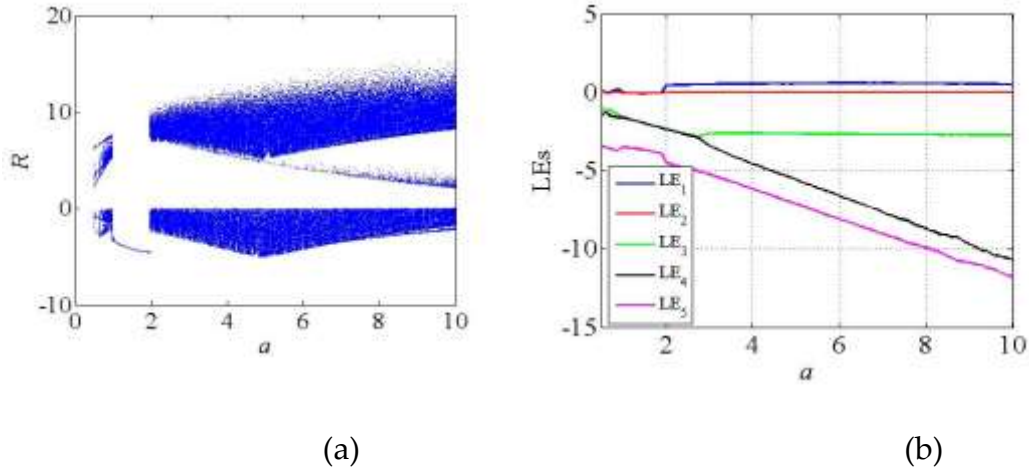


Figure 2 (a) BD and (b) LE spectra with respect to the parameter a .

Figure 2 presents a comprehensive analysis of the dynamic behavior of the N5DCSCM (3) through the BD and the corresponding LE spectra as functions of the system parameter a . In Figure 2a, the BD reveals a high-density region within the range $2 < a < 10$, characterized by a complex and scattered distribution of trajectory points. This dense and irregular pattern is a hallmark of chaotic dynamics, indicating that the system exhibits aperiodic and unpredictable behavior in this parameter range. Complementing this, Figure 2b displays the LE spectra for the same variation in parameter a , where the presence of positive LE values in the interval $2 < a < 10$ confirms the onset of chaos within this parameter regime.

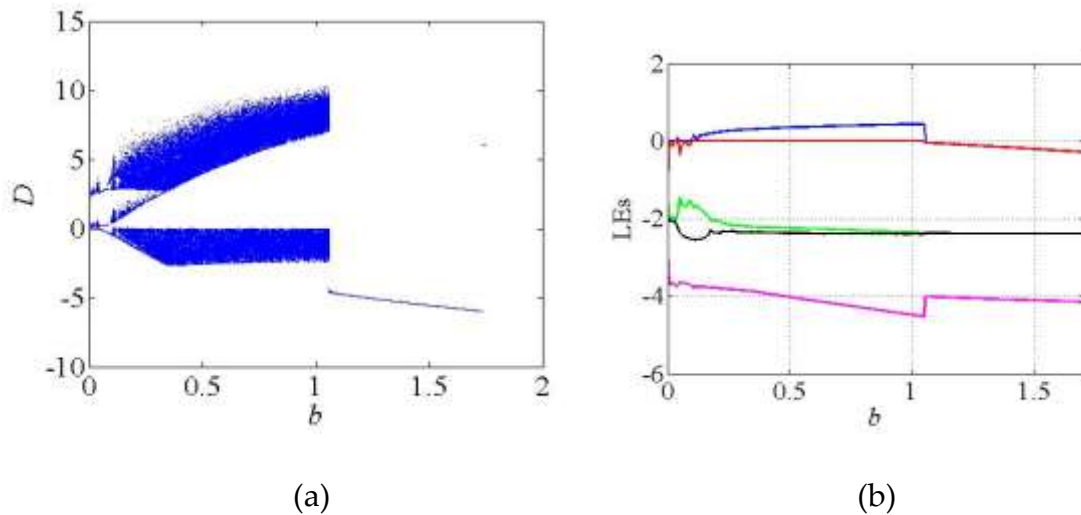


Figure 3 (a) BD and (b) LE spectra with respect to the parameter ' b '.

Figure 3 shows the bifurcation plot and the corresponding LE spectra of the N5DCSCM (3) as the function of the parameter b . Figure 3a clearly reveals that the chaotic dynamics occurs in the region $0 < b < 1.1$ as evidenced by dense and scattered trajectories in the bifurcation plot. Beyond this region, the system undergoes a transition to a stable state, represented by a single continuous line, indicating the convergence of trajectories. This observation is further supported by the corresponding LE spectra shown in Figure 3b, where the occurrence of positive LE values in the region $0 < b < 1.1$ conform the sensitivity to initial conditions and the existence of chaotic behaviour in the system.

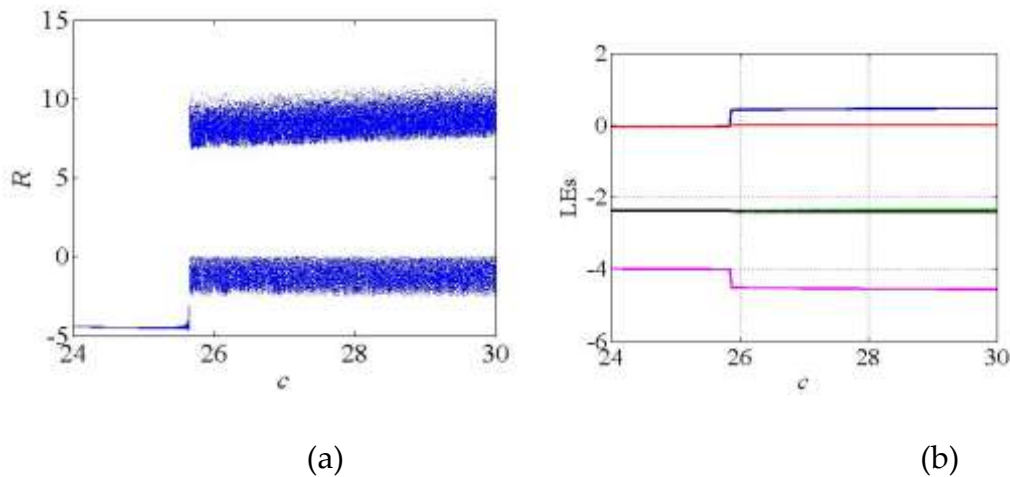


Figure 4 (a) BD and (b) LE spectra with respect to the parameter c .

Figure 4 shows the BD and LE spectra of the N5DCSCM (3) as a function of the parameter c in the region $24 < c < 30$. As illustrated in Figure 4a, the BD displays a single distinct line within the region $24 < c < 25.8$, indicating that the system displays stable and periodic behaviour in this region. However, as the parameter c exceeds $c = 25.8$, the system undergoes a bifurcation, leading to a transition into chaotic dynamics characterized by the appearance of two branches, which signify the onset of complex and, aperiodic behavior. Figure 4b presents the LE spectra corresponding to the variation of the parameter c , providing additional supports of the behaviour observed in the bifurcation diagram. In the region $24 < c < 25.8$, both LE_1 and LE_2 are zero while the remaining LEs are negative, indicating a stable and periodic behaviour of the system in this region. Beyond $c = 25.8$, LE_1 becomes positive while other exponents retain its polarity, clearly indicating the transition to chaotic behaviour in the specified region.

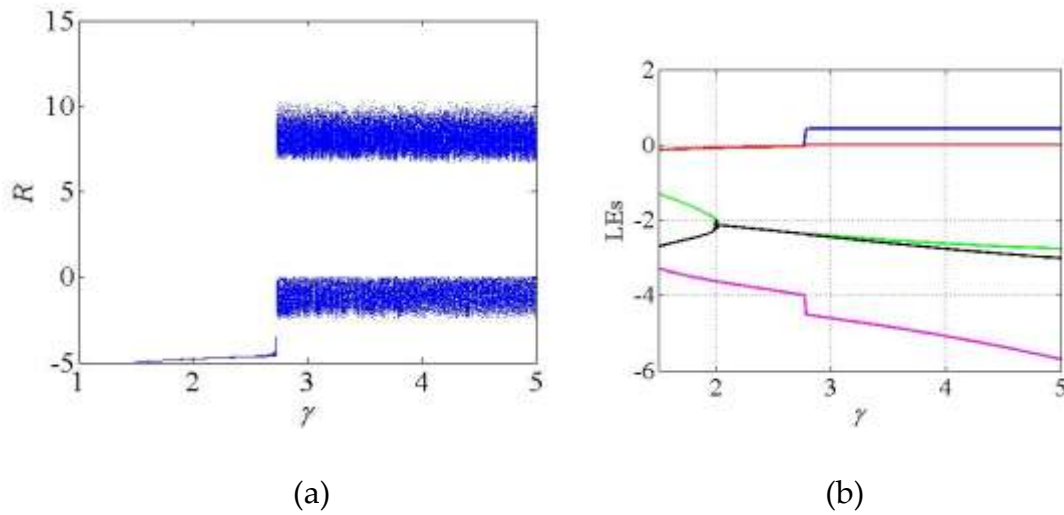


Figure 5 (a) BD and (b) LE spectra with respect to the parameter γ .

Figure 5a illustrates the BD of N5DCSCM (3) as the parameter γ varies over the interval $1 < \gamma < 5$. In the range $1 < \gamma < 2.7$, the diagram displays a single line, indicating that the system behaves in a stable and periodic manner with no significant sensitivity to initial conditions. However, as γ exceeds 2.7, the system undergoes a bifurcation, evidenced by the emergence of two distinct branches in the diagram. This bifurcation marks the beginning of complex dynamical behavior and signifies the onset of chaos. Supporting this observation, Figure 5b presents the corresponding LE spectra, where LE_1 remains non-positive for $\gamma < 2.7$, consistent with stable dynamics. Beyond $\gamma = 2.7$, LE_1 becomes positive, clearly indicating a transition to chaotic behavior. The presence of a positive LE_1 confirms sensitivity to initial conditions and reinforces the conclusion that the system enters a chaotic regime as the parameter γ increases past this critical threshold.

2.3.1 Multistability Analysis

Multistability refers to the presence of two or more stable states (attractors) under the same system parameters. A bifurcation diagram reveals multistability when multiple distinct attractor responses coexist at the same parameter value, visible by running the system from different initial conditions and plotting all steady-state outcomes. Multiple branches or scattered points at the same parameter value from different initial conditions are a signature of multistability.

In this section, the multistability is realized in the N5DCSCM (3) by plotting the bifurcation diagram for the parameter d with the initial conditions $(0.04, 0.04, 0.04, 0.04, 0.04)$ (blue) and $(-0.04, -0.04, -0.04, -0.04, 0.04)$ (red). Figure 6a reveals two distinct branches shown in blue and red within the interval $0 < d < 1.49$, indicating the presence of multiple coexisting periodic attractors. Additionally, the overlapped regions with scattered points within the interval $1.5 < d < 5$ suggest the existence of chaotic coexisting attractors in the N5DCSCM (3). Figure 6b further confirms that the N5DCSCM (3) exhibits chaotic dynamics with in the interval $1.5 < d < 5$, as indicated by one positive LE value. Figure 7 shows the multiple coexisting periodic and chaotic attractors at $d = 1.45$ and $d = 1.5$ respectively.

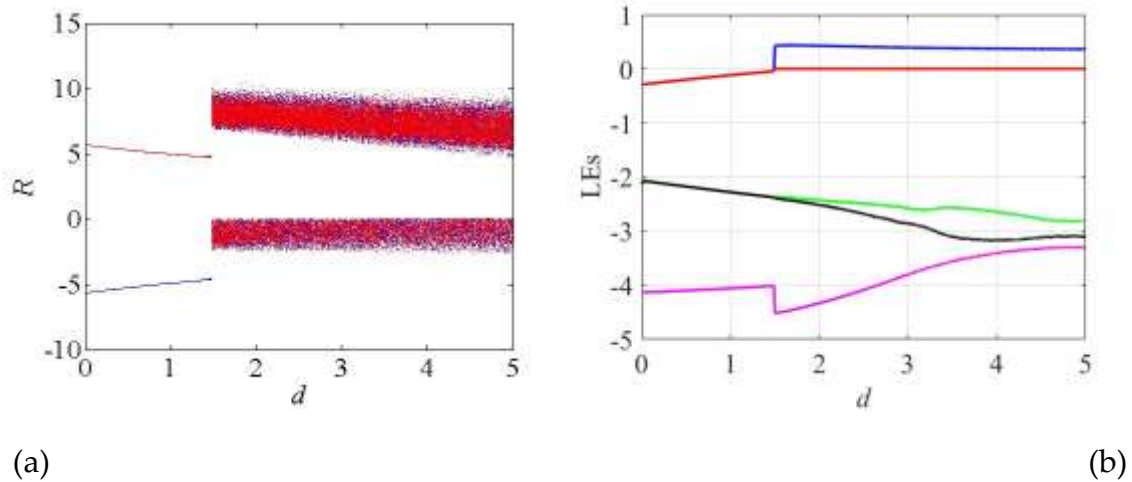


Figure 6 (a) BD and (b) LE spectra with respect to the parameter d .

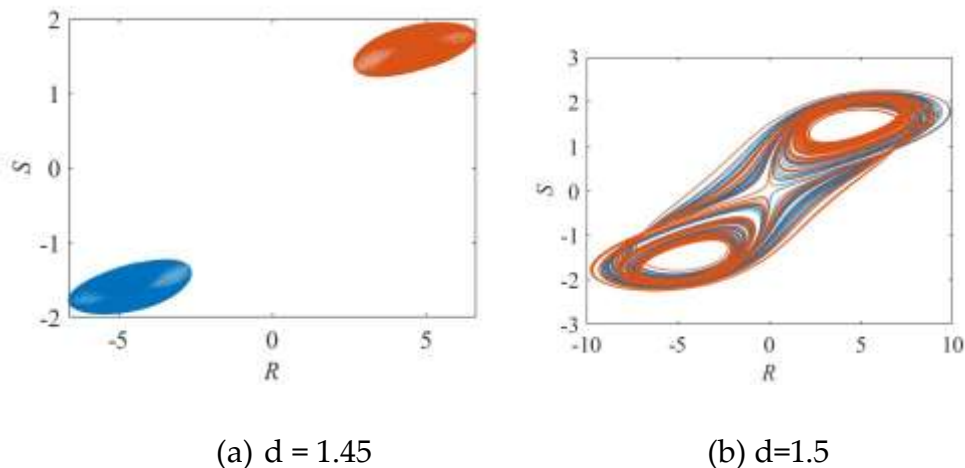


Figure 7 (a-b) Coexisting attractors in periodic and chaotic regions of the parameter d respectively.

2.3.2 Complete Amplitude Control via Rescaling

Complete amplitude control (CAC) in a chaotic system refers to the ability to systematically regulate the amplitude of chaotic oscillations without eliminating the

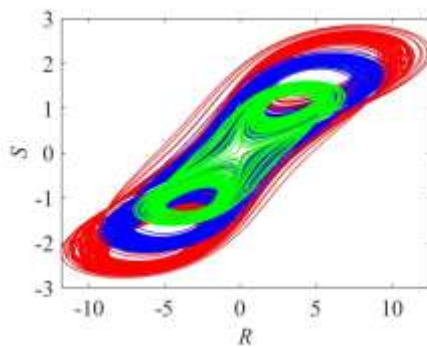
chaotic nature itself. CAC can be introduced into a chaotic system by modifying its dynamics with a constant control parameter that regulates the amplitude without eliminating chaos. Rescaling variables using a constant control parameter (k) is an effective method to achieve CAC in chaotic systems.

Consider the general system $\dot{x} = f(x)$, where $x \in \mathbb{R}^n$ is the state vector and $f(x)$ define nonlinear chaotic dynamics. Now, introduce a constant control parameter $k > 0$ to rescale the variables: $x = kX$, where X is the new rescaled variable. By differentiating $x = kX$, we will get

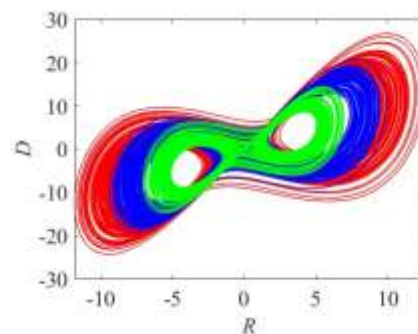
$$\begin{aligned}\dot{x} &= k\dot{X} = f(kX) \\ \dot{X} &= \frac{1}{k} f(kX)\end{aligned}$$

The shape and type of attractor remain unchanged, but the amplitude is scaled by k . The system's amplitude can be amplified by choosing $0 < k < 1$ and reduce it if $k > 1$.

Now consider the N5DCSCM (3) and apply rescaling transformation to all the state variables using k , such that $R = kR, D = kD, M = kM, C = kC, S = kS$. Substituting these into N5DCSCM (3) and simplifying, the scaled system is obtained which corresponds to Eq. (7).



(a)



(b)

$$C = - -$$

$$R \quad \gamma S$$

$$S = - +$$

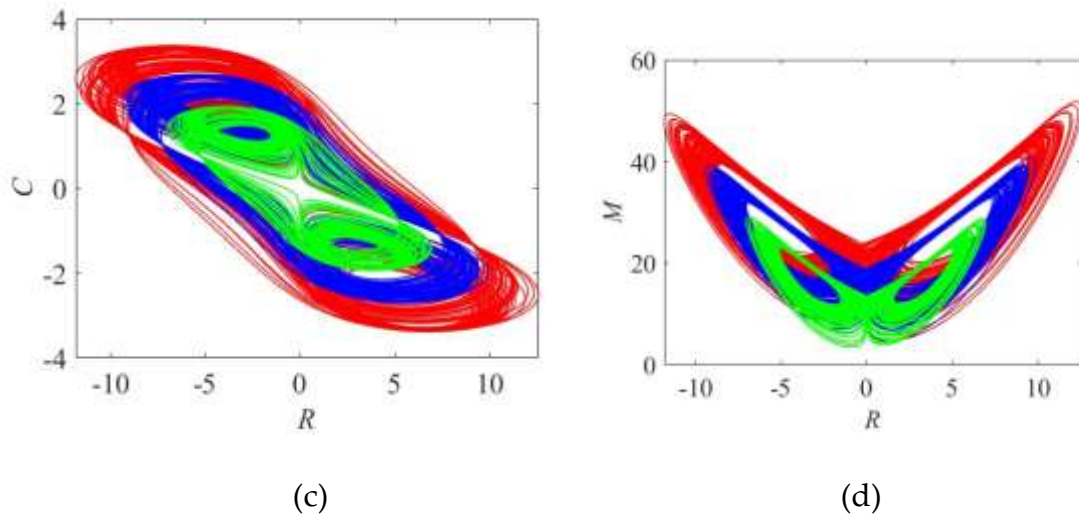


Figure 7 (a-d) Chaotic attractors of the rescaled system (7) in various 2D planes with $k = 0.8$ (red) and $k = 1.4$ (green).

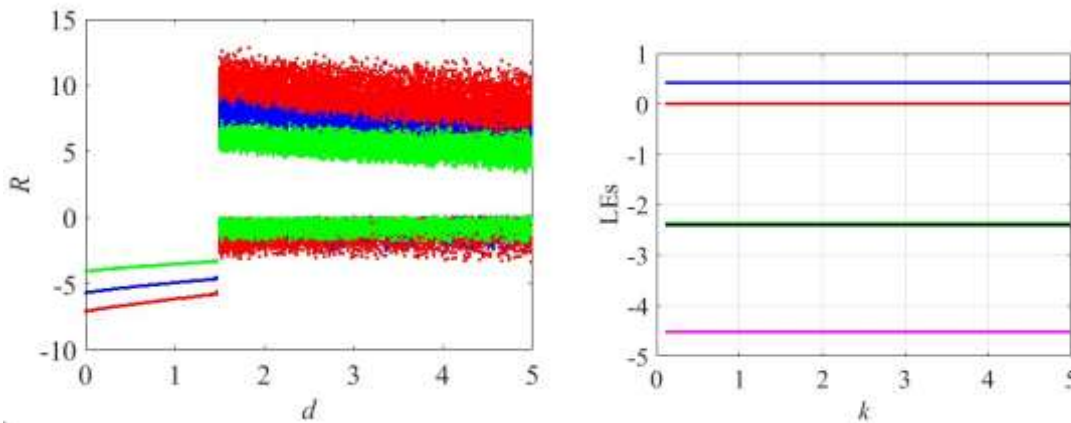


Figure 8 (a) BD with various k (b) LE spectra of the rescaled model (7) as a function of k .

Figure 7 shows chaotic attractors of the rescaled system (7) in various 2D planes for two values of the control parameter: $k = 0.8$ (red) and $k = 1.4$ (green). Figure 8a presents the BD of rescaled system (7) as a function of d again for $k = 0.8$ (red) and $k = 1.4$ (green). From both Figure 7 and Figure 8a, it is evident that control parameter k influences the amplitude of all the state variables: when k is fractional, it amplifies the amplitude; when k is non - fractional, it reduces the amplitude. Figure 8b, which shows the constant LE spectra, confirms that the LE values of the rescaled model (7) closely matched those of the N5DCSCM (3). It indicates that the chaotic nature of the proposed model is remains unaffected by the variation in the parameter k .

2.3.3 Offset Boosting Control

Offset boosting in chaotic systems refers to the technique of adding a constant parameter (an offset) to one or more state equations of a chaotic system. This method modifies the system's trajectory in phase space without changing its underlying dynamics, such as chaos, periodicity, or bifurcations. In this section, the trajectory of the N5DCSCM (3) is shifted in phase space along the S and C directions by introducing constant offsets u and v , respectively. The offset boosted model is formally expressed in Eq. (8).

$$\begin{cases} \dot{R} = a(D - R) + dC + S + u \\ \dot{D} = cR - RM - D \\ \dot{M} = RD - bM \\ \dot{C} = -R - aC \\ \dot{S} = -R + \gamma(S + u) \end{cases} \quad (8)$$

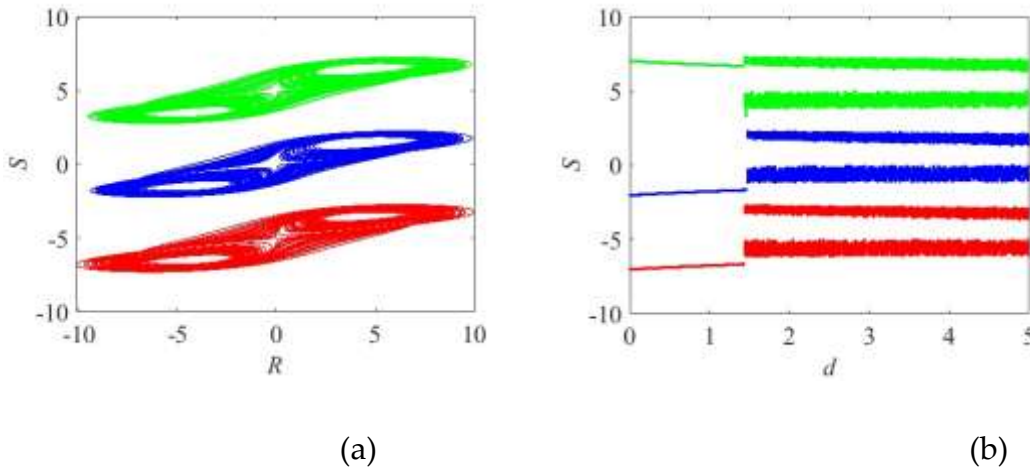


Figure 9 (a) Offset boosted attractor (b) BD of the model (8) with $u = 5$ (red) and $u = -5$ (green).

Figure 9a shows the offset boosted attractor of the model (8) along the direction of S , illustrating that the booster induces a positive shift in the signal for $u < 0$ and negative shift for $u > 0$. This behaviour is further validated through the BD depicted in Figure 9b, which plot the parameter d against the variable S .

2.4 Fuzzy logic-based controller design

The fuzzy logic controller operates by translating real-world inputs—such as product demand, supply levels, or production rates—into linguistic terms like “high,” “medium,” or “low.” These inputs are then processed using a set of pre-defined fuzzy rules created based on expert knowledge. Each rule follows a simple logic format, such as: “If demand is high and inventory is low, then increase production.” Using the Mamdani inference method, the controller evaluates all

relevant rules and combines their outcomes to determine an appropriate control action.

Afterward, the fuzzy output (still in linguistic form) is converted back into a precise numerical value through a process called defuzzification, which is then used to adjust variables within the supply chain system—such as production rate or shipment size. This approach allows the controller to make smooth, human-like decisions even in the presence of complex, nonlinear, or uncertain behaviors that are typical in chaotic supply chains.

In order to design a simple fuzzy controller, which can drive the convergence of chaotic system states towards zero. This stub control consists of simple fuzzy rules and its convergence speed is acceptable. The design of the fuzzy controller is illustrated in Eq. (4)

$$\begin{cases} \dot{R} = a(D - R) + dC + \alpha S + U_R \\ \dot{D} = cR - RM - D + U_D \\ \dot{M} = RD - bM + U_M \\ \dot{C} = -R - aC + U_C \\ \dot{S} = \gamma R - \delta S + U_S \end{cases} \quad (9)$$

Which U_R, U_D, U_M, U_C, U_S are inputs control. If the initial conditions are

$[R_0, D_0, M_0, C_0, S_0]^T = [0.04, 0.04, 0.04, 0.04, 0.04]^T$ and also the system parameters

are $\alpha = 1, \gamma = 2.8, \delta = 1, a = 2, b = 1.05, c = 26, d = 1.5$. Figure 10 illustrates the dynamic behavior of the system (9) over a 60-second simulation period under uncontrolled conditions, where all control inputs are set to zero. The trajectories of the state variables—retailer demand (R), distributor supply (D), manufacturer production (M), customer received product (C), and supply chain stress or distortion (S)—exhibit strong oscillations and irregular patterns, particularly visible in variables M and D, which fluctuate with high amplitude and frequency.

Now, the FC design method is described. The design steps are summarized as follows:

Step 1: Determine the error and error derivative

Step 2: Determine the type of membership function (for input and output)

Step 3: Number of membership functions (for input and output)

Step 4: Determine the fuzzy rules (for input and output)

Step 5: Relationship between rules or weighting (for input and output)

Step 6: Determine the fuzzy inference engine

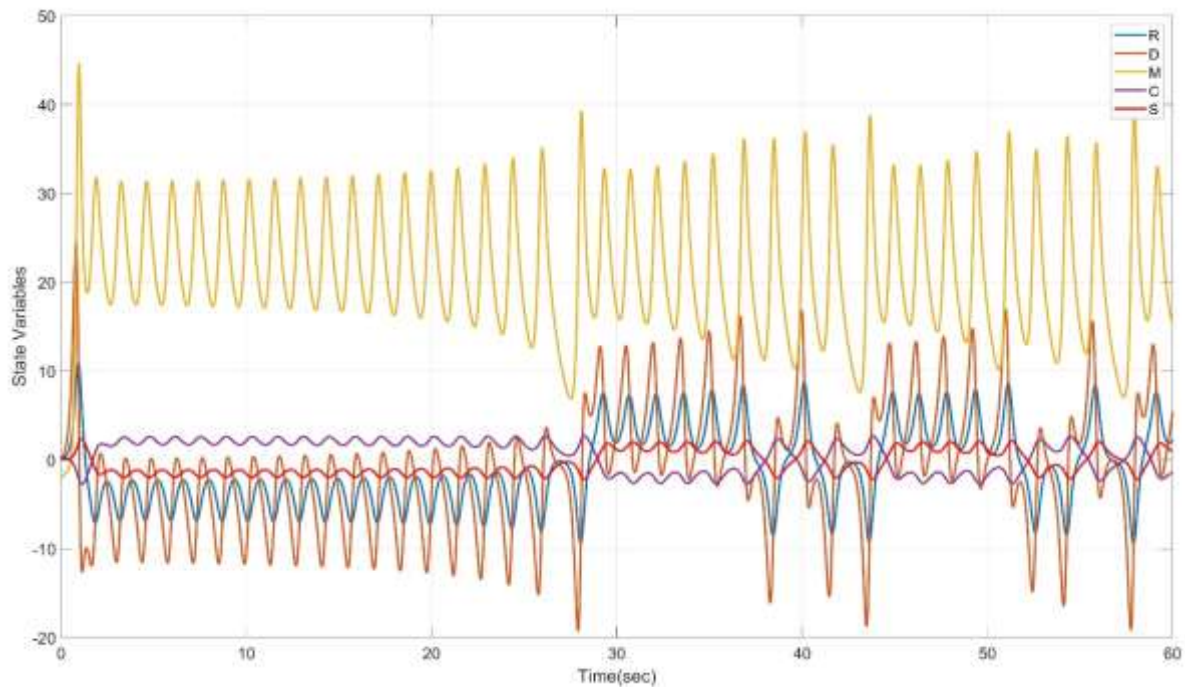


Figure 10. Time response of the chaotic equations of the Eq. (9)

Figure 11 illustrates that the proposed fuzzy control system takes the error and its derivative as inputs, which represent the deviation from the desired system behavior and the rate of that deviation, respectively. These inputs are processed through a Mamdani-type inference engine to generate the appropriate control signal. The output of the fuzzy system determines the control action needed to adjust the chaotic supply chain system toward a more stable and synchronized state.

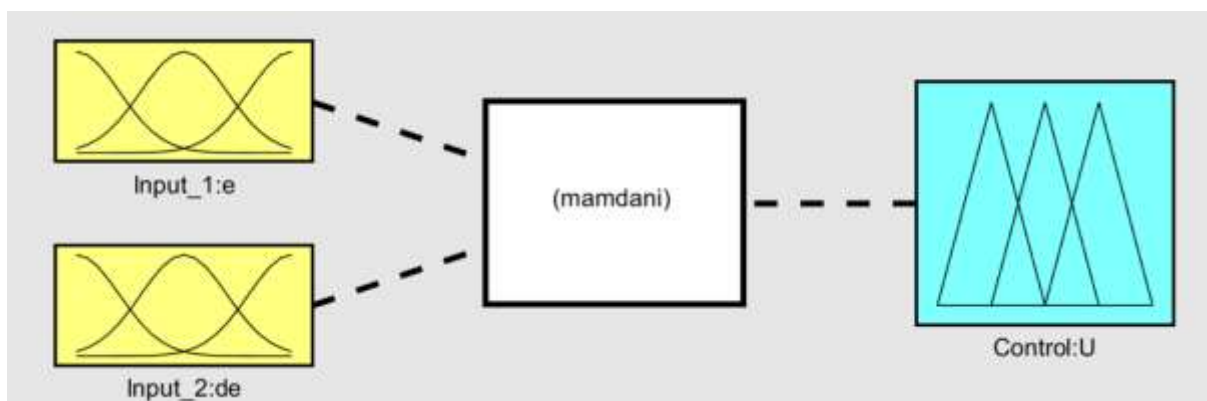


Figure 11. Fuzzy controller design structure

The membership functions in the proposed fuzzy system are defined using a triangular shape, with three membership functions assigned to each input and

output variable. As shown in Figure 12, these functions help map the input-output relationships within the fuzzy controller. The rule base is constructed with equal weighting (set to 1) for each rule, ensuring balanced influence across all control actions. The fuzzy rules developed for the system (9) are detailed as follows.

IF Error is P and d_Error P, THEN U_Fuzzy is P

IF Error is P and d_Error Z, THEN U_Fuzzy is P

IF Error is P and d_Error N, THEN U_Fuzzy is Z

IF Error is Z and d_Error P, THEN U_Fuzzy is P

IF Error is Z and d_Error Z, THEN U_Fuzzy is Z

IF Error is Z and d_Error N, THEN U_Fuzzy is N

IF Error is N and d_Error P, THEN U_Fuzzy is Z

IF Error is N and d_Error Z, THEN U_Fuzzy is N

IF Error is N and d_Error N, THEN U_Fuzzy is N

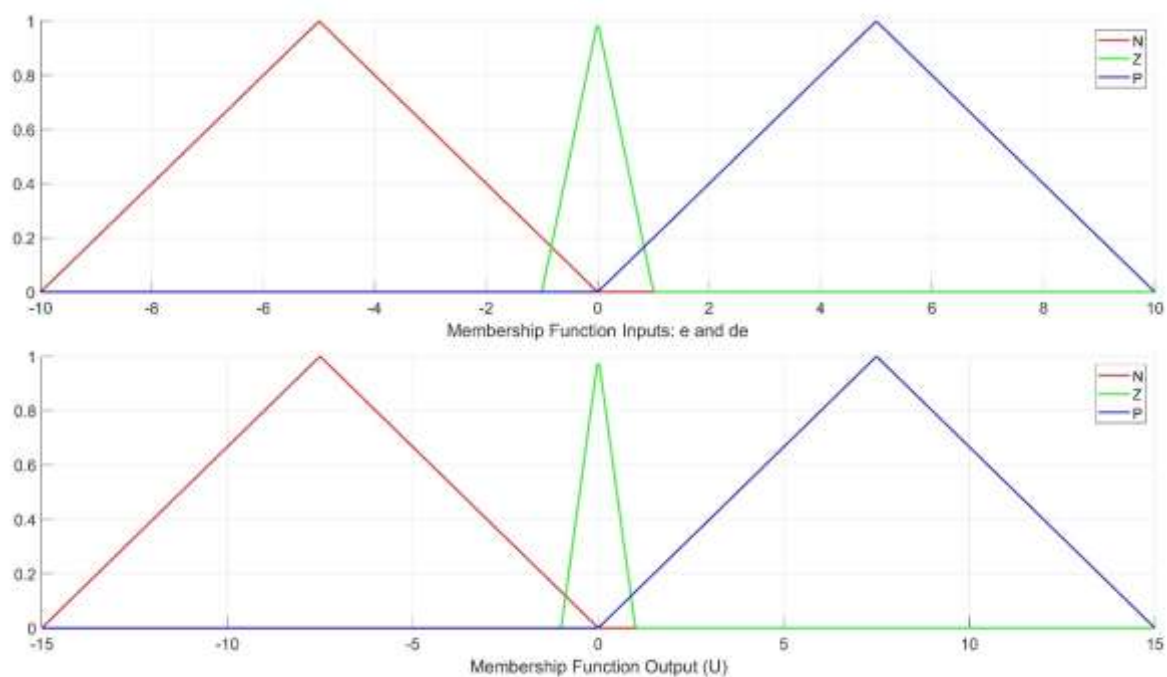


Figure 12. Membership functions for input and output

Figure 12 displays the triangular membership functions used for both the inputs and output of the fuzzy logic controller. The top plot shows the membership

functions for the input variables—error (eee) and change in error (dedede)—which are categorized into three linguistic terms: Negative (N), Zero (Z), and Positive (P). Similarly, the bottom plot represents the output control signal (UUU), also defined by the same three linguistic labels. These triangular membership functions enable the fuzzy inference system to interpret input variations and generate smooth control outputs. The symmetry and simplicity of the triangular shape ensure computational efficiency while effectively capturing the behavior of the chaotic supply chain system.

The Table 1 presented is a Fuzzy Rule Table, which defines the control actions for a fuzzy logic controller based on two input variables: Error and d_Error (change in error). The table uses linguistic variables—P (Positive), Z (Zero), and N (Negative)—to categorize the input values. The rows represent the Error values, while the columns represent the rate of change of the error (d_Error). The intersecting cells indicate the control output or fuzzy action (U_Fuzzy) that should be taken by the controller based on the combination of these inputs. For example, when both Error and d_Error are Positive (P), the output is also Positive (P), suggesting a strong corrective action in the same direction.

Table1: Fuzzy rules: P=Positive, Z=Zero, N=Negative

U_Fuzzy		d_Error		
		P	Z	N
Error	P	P	P	Z
	Z	P	Z	N
	N	Z	N	N

Table 1 is an essential part of fuzzy logic systems, particularly in control applications like robotics, process control, or temperature regulation, where precise mathematical models are difficult to derive. The logic embedded in this table mimics human reasoning by applying intuitive control decisions. For instance, if the error is Negative and the rate of change is also Negative (indicating the error is getting worse in the negative direction), the controller responds with a Negative output, maintaining the correction direction. Such a rule base helps smooth system behavior and improves responsiveness without overshooting or instability.

2.5 Numerical simulations

In the previous section, the basic structure of the fuzzy controller was described. Now, in this section, the numerical simulation results will be depicted. In the numerical simulation, the system parameters are $[R_0, D_0, M_0, C_0, S_0]^T = [0.04, 0.04, 0.04, 0.04, 0.04]^T$, respectively, and the initial

conditions are $\alpha = 1, \gamma = 2.8, \delta = 1, a = 2, b = 1.05, c = 26, d = 1.5$. The controller has been applied to the hyperchaotic system since time $T=35\text{sec}$. So, there is no control before this time.

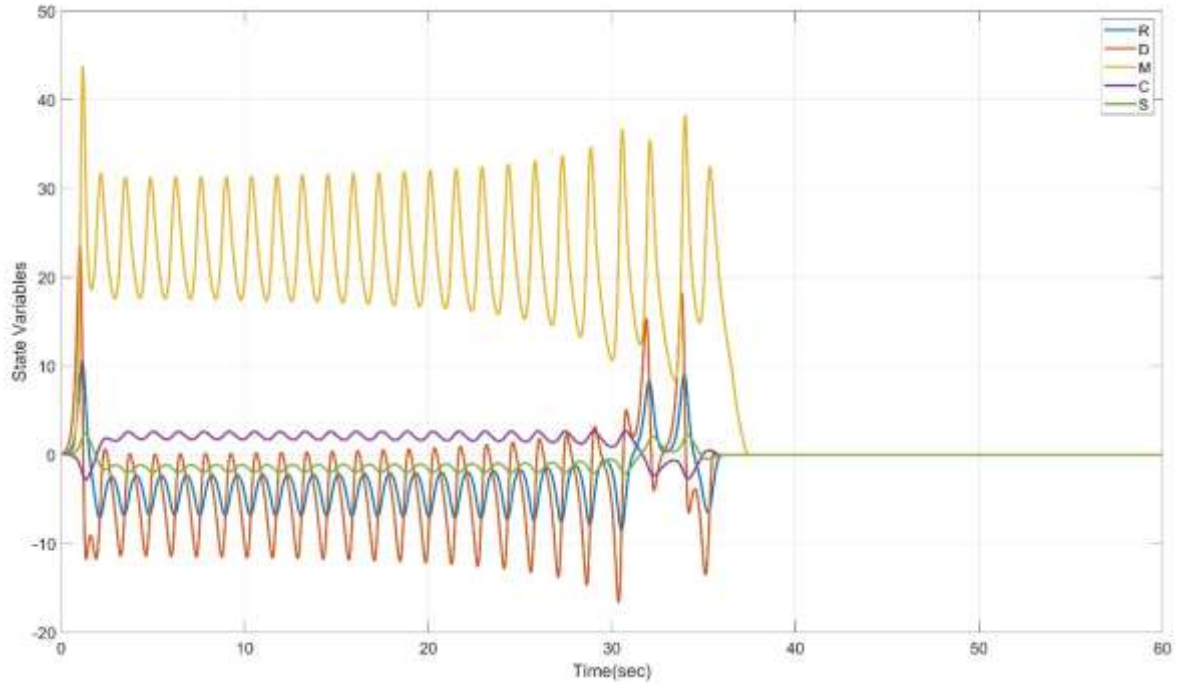


Figure 13. Time response of the SCM before and after the proposed fuzzy controller.

Figure 13 demonstrates the effectiveness of the fuzzy logic controller in stabilizing the CSCM. However, once the controller is activated around the 30-second mark, the system rapidly converges to equilibrium. Within a short period, all state variables settle to zero, indicating that the controller successfully suppresses the chaotic dynamics and drives the system toward a stable, synchronized state. This highlights the controller's ability to efficiently regulate supply chain fluctuations and achieve steady performance. The control signal condition in Figure 14 shows that it has a small amplitude and is also free of oscillations. This indicates that it has the potential to be implemented in the real world. In the next part of the simulation, the hyperchaotic system is subjected to an unknown input. This unknown input is equal to $|\Delta|=0.2$ and will be added to all rows of the system (9). In other words, the hyperchaotic equations (9) will be as follows.

$$\begin{cases} \dot{R} = a(D - R) + dC + \alpha S + U_R + 0.2R \\ \dot{D} = cR - RM - D + U_D + 0.2D \\ \dot{M} = RD - bM + U_M + 0.2M \\ \dot{C} = -R - aC + U_C + 0.2C \\ \dot{S} = \gamma R - \delta S + U_S + 0.2S \end{cases} \quad (10)$$

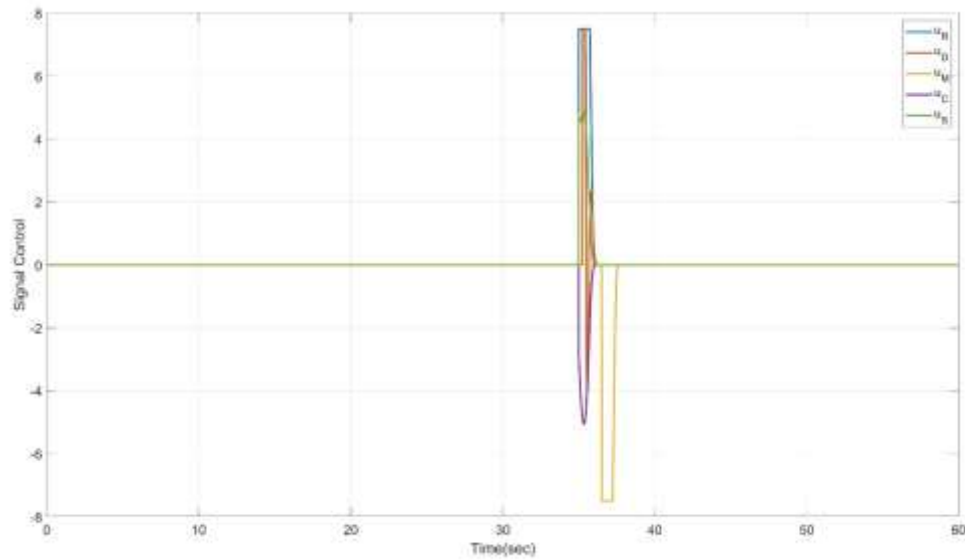


Figure 14. Time response of the proposed fuzzy controller.

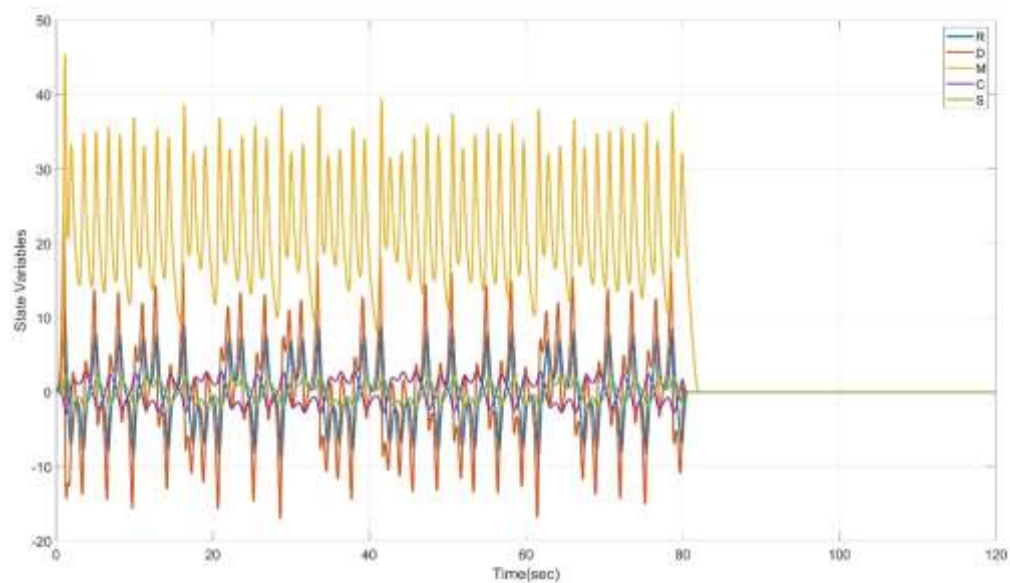


Figure 15. Time response of model (10) with unknown input before and after applying the proposed fuzzy controller.

Figure 15 illustrates the time response of the enhanced N5DCSCM when subjected to an unknown external input, both before and after applying the proposed fuzzy logic controller. Initially, the system exhibits significant instability due to the presence of the unknown input, as indicated by the erratic and high-amplitude oscillations in the state variables. However, after the FC is activated, the trajectories of all state variables—including demand, supply, production, and distortion—begin to stabilize and gradually converge towards zero. This transition confirms the controller's effectiveness in mitigating the impact of external disturbances and driving the chaotic system towards a synchronized and steady state.

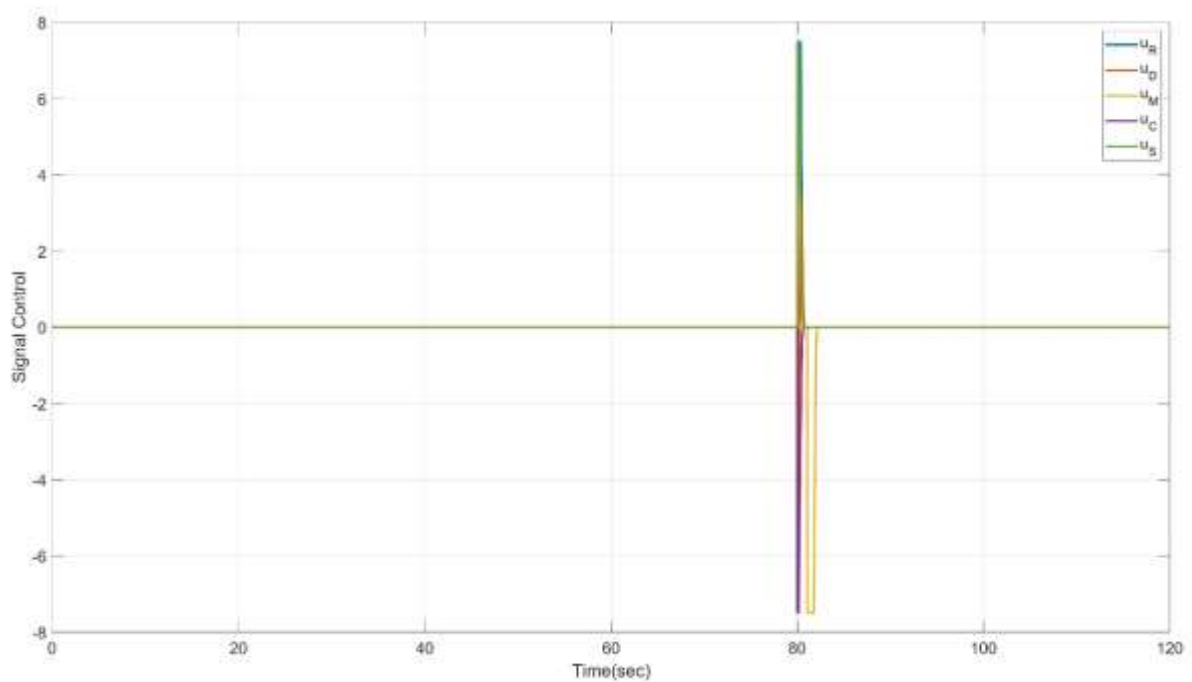


Figure 16 Time response of the proposed fuzzy controller in the presence of unknown input

Figure 16 complements this observation by showing the behavior of the control signal generated by the fuzzy controller in response to the unknown input. The figure reveals that the control signal maintains a low amplitude and is free from oscillations, which implies an efficient and energy-conserving control action. As the system becomes more stable over time, the control signal diminishes smoothly to zero, indicating that the controller not only suppresses chaos effectively but also does so with minimal effort.

2.6 Conclusion

This study introduces a N5DCSCM that integrates market shock dynamics into a previously established four-tier system. Through rigorous dynamical analysis—including BD, LE spectra, and multistability exploration—the model reveals rich

and complex behaviors such as chaos and coexisting attractors. The inclusion of market shock parameters enables a more realistic simulation of disruptions in real-world supply chains. To address the instability arising from chaotic dynamics, advanced control mechanisms were proposed, including complete amplitude control via rescaling and offset boosting to manipulate phase trajectories without suppressing chaos. Most notably, a fuzzy logic-based controller was developed using a Mamdani inference engine. Numerical simulations demonstrate that this controller effectively stabilizes the N5DCSCM with minimal oscillations and robust performance—even in the presence of unknown external inputs. The findings confirm that the proposed model and control strategy provide a good performance and adaptable framework for understanding and managing complex supply chains under uncertainty, with significant potential for real-world applications in logistics and operations management.

2.7 References

- [1] Heeß, P., Rockstuhl, J., Körner, M. F., & Strüker, J. (2024). Enhancing trust in global supply chains: Conceptualizing Digital Product Passports for a low-carbon hydrogen market. *Electronic Markets*, 34(1), 10.
- [2] Allan, B. B., & Nahm, J. (2025). Strategies of green industrial policy: How states position firms in global supply chains. *American political science review*, 119(1), 420-434.
- [3] Al Bashar, M., Taher, M. A., Islam, M. K., & Ahmed, H. (2024). The impact of advanced robotics and automation on supply chain efficiency in industrial manufacturing: a comparative analysis between the us and Bangladesh. *Economics, Development & Project Management*, 3(03), 28-41.
- [4] Rolf, B., Jackson, I., Müller, M., Lang, S., Reggelin, T., & Ivanov, D. (2023). A review on reinforcement learning algorithms and applications in supply chain management. *International Journal of Production Research*, 61(20), 7151-7179.
- [5] Bednarski, L., Roscoe, S., Blome, C., & Schleper, M. C. (2025). Geopolitical disruptions in global supply chains: a state-of-the-art literature review. *Production planning & control*, 36(4), 536-562.
- [6] Lim, M. K., Li, Y., Wang, C., & Tseng, M. L. (2021). A literature review of blockchain technology applications in supply chains: A comprehensive analysis of themes, methodologies and industries. *Computers & industrial engineering*, 154, 107133.
- [7] Ivanov, D., Dolgui, A., & Sokolov, B. (2022). Cloud supply chain: Integrating Industry 4.0 and digital platforms in the "Supply Chain-as-a-Service". *Transportation Research Part E: Logistics and Transportation Review*, 160, 102676.
- [8] Mohsen, B. M. (2023). Impact of artificial intelligence on supply chain management performance. *Journal of Service Science and Management*, 16(1), 44-58.
- [9] Nahr, J. G., Nozari, H., & Sadeghi, M. E. (2021). Green supply chain based on artificial intelligence of things (AIoT). *International Journal of Innovation in Management, Economics and Social Sciences*, 1(2), 56-63.
- [10] Ivanov, D. (2023). Intelligent digital twin (iDT) for supply chain stress-testing, resilience, and viability. *International Journal of Production Economics*, 263, 108938.
- [11] Agca, S., Babich, V., Birge, J. R., & Wu, J. (2022). Credit shock propagation along supply chains: Evidence from the CDS market. *Management Science*, 68(9), 6506-6538.

-
- [12] Davis, K. F., Downs, S., & Gephart, J. A. (2021). Towards food supply chain resilience to environmental shocks. *Nature Food*, 2(1), 54-65.
- [13] Hadachek, J., Ma, M., & Sexton, R. J. (2024). Market structure and resilience of food supply chains under extreme events. *American Journal of Agricultural Economics*, 106(1), 21-44.
- [14] Dou, S., Zhu, Y., Liu, J., & Xu, D. (2024). The power of mineral: Shock of the global supply chain from resource nationalism. *World Development*, 184, 106758.
- [15] Diaz, E. M., Cunado, J., & de Gracia, F. P. (2024). Global drivers of inflation: The role of supply chain disruptions and commodity price shocks. *Economic Modelling*, 140, 106860.
- [16] Xie, Q., Jiang, Y., Jia, N., & Wang, H. (2024). Asymmetric impact of oil structural shocks on non-ferrous metals supply chains: A groundbreaking multidimensional quantile-on-quantile regression. *International Review of Financial Analysis*, 96, 103607.
- [17] Lafrogne-Joussier, R., Martin, J., & Mejean, I. (2022). Supply shocks in supply chains: Evidence from the early lockdown in China. *IMF economic review*, 71(1), 170.
- [18] Hendricks, K. B., Jacobs, B. W., & Singhal, V. R. (2020). Stock market reaction to supply chain disruptions from the 2011 Great East Japan Earthquake. *Manufacturing & Service Operations Management*, 22(4), 683-699.
- [19] Costello, A. M. (2020). Credit market disruptions and liquidity spillover effects in the supply chain. *Journal of Political Economy*, 128(9), 3434-3468.
- [20] Bhattacharya, A., Geraghty, J., Young, P., & Byrne, P. J. (2013). Design of a resilient shock absorber for disrupted supply chain networks: a shock-dampening fortification framework for mitigating excursion events. *Production Planning & Control*, 24(8-9), 721-742.
- [21] Johansyah, M. D., Sambas, A., Farman, M., Vaidyanathan, S., Zheng, S., Foster, B., & Hidayanti, M. (2024). Global mittag-leffler attractive sets, boundedness, and finite-time stabilization in novel chaotic 4d supply chain models with fractional order form. *Fractal and Fractional*, 8(8), 462.
- [22] Johansyah, M. D., Vaidyanathan, S., Sambas, A., Benkouider, K., Hamidzadeh, S. M., & Hidayanti, M. (2024). Dynamical Analysis and Sliding Mode Controller for the New 4D Chaotic Supply Chain Model Based on the Product Received by the Customer. *Mathematics*, 12(13), 1938.

-
- [23] Peng, Y., & Wu, J. (2024). Impulse synchronization strategy for supply chains considering combined effects and demand saturation. *Computers & Industrial Engineering*, 198, 110696.
- [24] Sepestanaki, M. A., Rezaee, H., Soofi, M., Fayazi, H., Rouhani, S. H., & Mobayen, S. (2024). Adaptive continuous barrier function-based super-twisting global sliding mode stabilizer for chaotic supply chain systems. *Chaos, Solitons & Fractals*, 182, 114828.
- [25] Bhat, S. A., Aljuneidi, T., & Li, Z. (2024). Dynamic Analysis of an Economic and Financial Supply Chain System Using the Supervised Neural Networks. *IEEE Access*, 12, 95901-95913.
- [26] Aslam, M. S., Bilal, H., Band, S. S., & Ghasemi, P. (2024). Modeling of nonlinear supply chain management with lead-times based on Takagi-Sugeno fuzzy control model. *Engineering applications of artificial intelligence*, 133, 108131.
- [27] Liu, Z., Jahanshahi, H., Gómez-Aguilar, J. F., Fernandez-Anaya, G., Torres-Jiménez, J., Aly, A. A., & Aljuaid, A. M. (2021). Fuzzy adaptive control technique for a new fractional-order supply chain system. *Physica Scripta*, 96(12), 124017.
- [28] Kocamaz, U. E., Taşkın, H., Uyaroğlu, Y., & Göksu, A. (2016). Control and synchronization of chaotic supply chains using intelligent approaches. *Computers & Industrial Engineering*, 102, 476-487.
- [29] Cao, E. Z., Peng, C., Xie, X., & Yang, Y. (2025). Hybrid Modeling and Fuzzy Control Via Petri Nets for Supply Chain Networks Under Disruptions. *IEEE Transactions on Fuzzy Systems*, 33(5), 1540-1554.
- [30] Xu, W., Yan-Min, J., & Hui, L. (2009, July). Prediction model of supply chain demand based on fuzzy neural network with chaotic time series. In *2009 IEEE/INFORMS International Conference on Service Operations, Logistics and Informatics* (pp. 675-680). IEEE.
- [31] Zhang, S., Zhao, X., & Zhang, J. (2014). Dynamic model and fuzzy robust control of uncertain closed-loop supply chain with time-varying delay in remanufacturing. *Industrial & Engineering Chemistry Research*, 53(23), 9805-9811.
- [32] Cuong, T. N., Kim, H. S., & You, S. S. (2023). Decision support system for managing multi-echelon supply chain networks against disruptions using adaptive fractional order control algorithm. *RAIRO-Operations Research*, 57(2), 787-815.

CHAPTER 3

Controlling the Unpredictable: Bifurcation and Backstepping Strategies in Supply Chain Dynamics

3.1 Introduction

Supply Chain Management (SCM) involves the coordination and integration of various activities and processes within a network of organizations that collaborate to deliver a product or service to the end customer [1]-[2]. The key entities in a supply chain typically include retailers, distributors, and manufacturers [3]-[4]. In summary, they play distinct but interconnected roles in the supply chain. Effective coordination and collaboration among these entities is essential for achieving efficiency, responsiveness, and customer satisfaction throughout the supply chain [5]-[6].

Several attribute properties within the SCMM defy adequate description through basic analysis. Therefore, it becomes imperative to engage in theoretical exploration of the complexity inherent in the supply chain system. This involves employing methods such as bifurcation and chaos control within the framework of nonlinear dynamics. Numerous studies have explored the manifestation of chaos in SCMM. For instance, Xu et al. [7] introduced an ASTSM control algorithm to address chaotic SCMM. The theory control can be extended to novel integration software for operational management within SCMM networks. Kocamaz et al. [8] demonstrated the control of a chaotic SCMM using ANN based controllers. They also presented the synchronization of two identical SCMM with distinct initial conditions using ANFIS technique. Göksu et al. [9] proposed the mathematical model of a control chaotic SCMM system, employing linear feedback controllers with Lyapunov stability theory. Nav et al. [10] investigated SCMM with a smooth ordering policy and introduced a new policy designed based on a proportional-derivative technique. Açıkgöz et al. [11] examined a three-dimensional SCMM, utilizing it to stabilize the system by introducing a linear control to increase production and prevent a collapse leading to dangerous instability. Chen and Zhou [12] developed a dynamic price and advertising game model for an omni-channel SCMM involving online purchases with in-store pickups. They explored the stability and complexity of migration rates for online and traditional consumers, as well as the sharing rate of advertising costs. Tian et al. [13] analyzed a Stackelberg dynamic model for a multi-channel SCMM, involving a manufacturer and two retailers. This study focused on a manufacturer providing a single product to traditional retailers, online retailers, and a direct channel. Peng et al. [14] proposed a novel SCMM sensitive to various uncertainties and exogenous disturbances. They

discussed the impulsive synchronization SCMMs with identical structures. Qian et al. [15] investigated a SCMM under technology subsidies, involving a general contractor and two green building material manufacturers. The research examined how individuals involved in the green building material industry make decisions related to technological innovation within the SCMM under a dynamic game. Han and Wang [16] explored the chaotic behaviors of nonlinear SCMM using control theory, nonlinear system theory, chaos theory, and confirmed through the Lyapunov exponent that the behavior of demand information-sharing SCMM members alternates between chaotic and periodic movement.

The primary hurdle in this domain involves formulating control and management strategies that guarantee the systems operate effectively. Control theory has laid a solid groundwork for addressing the complexities of nonlinear dynamics. Studies related to control in supply chain have been widely studied in the field of chaos such as fixed-time super-twisting sliding mode [17], robust H^∞ control [18], unidirectional and bidirectional [19], radial basis function [20], nonlinear control [21], ANFIS control [22], fuzzy adaptive control [23], delayed feedback control [24] and fault-tolerant control strategy [25]. Based on this literature, backstepping control is not reported for control strategy for the SCMM. In our study, backstepping control provides a systematic way to design controllers that are robust to uncertainties and disturbances in the system. The method allows for the incorporation of adaptive elements to adjust the controller parameters in real-time, enhancing the system's ability to cope with varying conditions.

In this paper, we assess the stability of the SCMM by identifying and analyzing key bifurcation points, including Hopf bifurcation, transcritical bifurcation, and double-zero bifurcation. Furthermore, we investigate the dynamical characteristics of the SCMM through the use of bifurcation diagrams and Lyapunov exponents, aiming to uncover periodic, chaotic, and reverse period-doubling behaviors. Finally, we proposed backstepping controllers to manage the chaotic behavior within the SCMM and achieve synchronization between two SCMMs.

The rest of this paper are structured as outlined below: Section 2 focuses on the modeling of the SCMM and the exploration of stability through bifurcation techniques. Moving to Section 3, the examination of dynamical analysis is conducted using Lyapunov exponents and bifurcation diagrams. In Section 4, a backstepping control scheme is implemented to manage behavior of the SCMM, and diverse numerical simulations are showcased. Lastly, Section 5 provides concluding remarks.

3.2 A Chaotic Supply Chain Model

In 2022, Hamidzadeh et al. [26] defined a chaotic model consisting of a three-tier supply chain network with retailers, distributors and manufacturers, which can be described as follows:

$$\begin{cases} \dot{y}_1 = y_2 \\ \dot{y}_2 = y_3 \\ \dot{y}_3 = ay_1 - by_2 - y_3 - y_1^2 \end{cases} \quad (1)$$

where y_1 is retailers, y_2 is distributors, and y_3 is manufacturers. The first differential equation in (1) describes the behavior of retailers that are affected by their sales and the response by distributors to these requests. The second differential equation in (2) describes the behavior of distributors who mainly seek to control their inventory levels and who will be constantly ordering from the factory. The third differential equation in (3) describes the behavior of manufacturers who are in direct contact with the retailers and distributors and the manufacturers produce the products with safety factors. In this equation, a and b are the satisfaction constants of the retailer and distributor of the manufacturer's products, respectively. System (1) exhibits chaotic behavior with parameter $a = 7.5$; $b = 3.8$ and the initial conditions are $y_1(0) = 1$, $y_2(0) = 1$, $y_3(0) = 1$.

Applying the results reported in [27], we obtain the following codim 1 bifurcation.

Proposition 2.1. Let $b > 0$ fixed. Then system (1) displays a Hopf bifurcation at the equilibrium point $O(0, 0, 0)$ when the parameter a pass through the critical value $a_0 = -b$.

In fact, the line $a + b = 0$, $b > 0$ is a Hopf curve of system (1) at O .

Proposition 2.2. Let $b > 0$ fixed. Then system (1) displays a Hopf bifurcation at the equilibrium point $E(a, 0, 0)$ when the parameter a pass through the critical value $a_0 = b$.

In fact, the line $a - b = 0$, $b > 0$ is a Hopf curve of system (1) at E .

Proposition 2.3. Let $b > 0$ fixed. Then system (1) displays a transcritical bifurcation when the parameter a pass through the critical value $a_0 = 0$.

In fact, the line $a = 0$, $b > 0$ is a transcritical bifurcation curve of system (1).

In addition, system (1) experiences a codim 2 bifurcation.

Proposition 2.4. System (1) displays a double-zero bifurcation when (a, b) passes through $(0, 0)$.

3.3 Dynamical Analysis

The dynamic traits of nonlinear systems demonstrate significant fluctuations based on the values assigned to their parameters. Transitioning from one behavior to another, termed bifurcation, may take place upon reaching specific parameter ranges. This study will delve into the complexity responses of the recently introduced system (1) through numerical computations, with variations in the parameters

a and b. In particular, we will analyze how the occurrence of local maxima in the signal x , denoted as

x_{\max} , evolves concerning the variations in the parameters a and b. These local maxima represent the highest points reached by the signal x over time for each specific value of a and b, offering insights into the system's dynamic behavior as the parameters are varied.

The Lyapunov exponent of a dynamical system is a measurable quantity that characterizes the rate of separation of infinitesimally close trajectories of the dynamical system in the phase space. A 3-D dynamical system has three Lyapunov exponents which can be arranged in non-increasing order as follows: $LE_1 \geq LE_2 \geq LE_3$. The 3-D dynamical system can be classified based on the following cases for the Lyapunov exponents:

- (a) Stable equilibrium point if all the Lyapunov exponents are negative.
- (b) Limit cycle if $LE_1 = 0$ and LE_2, LE_3 are negative.
- (c) A chaotic attractor if $LE_1 > 0, LE_2 = 0$ and $LE_3 < 0$.

In case (c), when a chaotic attractor exists for the 3-D dynamical system, the Kaplan-Yorke dimension of the system can be defined as

$$D_K = 2 + \frac{LE_1 + LE_2}{|LE_3|}. \quad (2)$$

3.4 Parameter a varying

By maintaining the values of b at 3.8, we can examine the impact of adjusting parameter a within the range of 4 to 7.5 on system (1). Figure 1 illustrates the Lyapunov exponent spectrum and the associated bifurcation diagram of system (1), revealing that the system exhibits both periodic and chaotic behavior as a increases within the [4, 7.5] range.

When the parameter a assumes values within the intervals ([4, 6.86], [7.04, 7.11], and 6.92), the dynamics of system (1) exhibit periodic behavior, as illustrated in Figure 2(a). This is corroborated by the presence of one zero Lyapunov exponent (LE) and two negative LEs. Specifically, these Lyapunov exponent values are as follows: $LE_1 = 0$, $LE_2 = -0.110$, and $LE_3 = -0.891$ (for $a = 6$).

For values of parameter a within the intervals ([6.86, 7.04], [7.11, 7.5]), the system (1) exhibits chaotic behavior, as depicted in Figure 2(b), accompanied by one positive Lyapunov exponent (LE). Specifically, the associated Lyapunov exponent values are found as follows: $LE_1 = 0.149$, $LE_2 = 0$, and $LE_3 = -1.151$ (for $a = 7.2$), and the system's Kaplan-Yorke dimension assumes a non-integer value of $D_K = 2.1295$.

Furthermore, the bifurcation diagram illustrated in Figure 1 indicates that the system (1) undergoes the well-known period-doubling route to chaos.

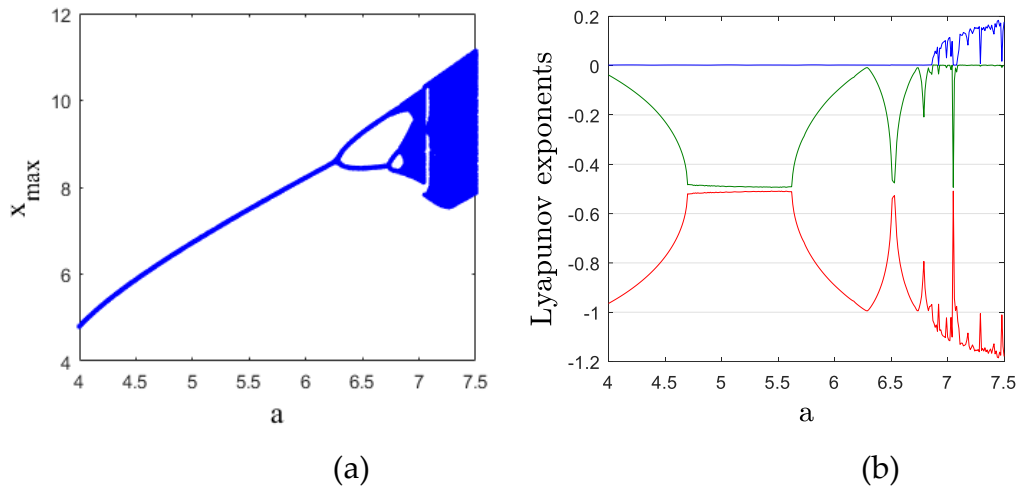


Fig 1: (a) Bifurcation diagram and (b) Lyapunov exponents spectrum of the system (1) when: $b=3.8$, and $a \in [4, 7.5]$.

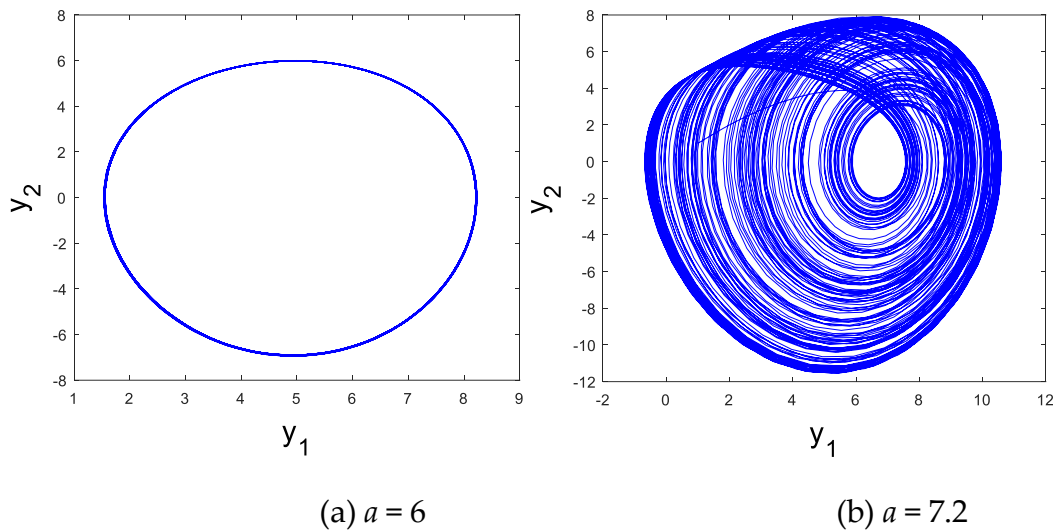


Fig. 2. Phase plots of system (1) for specific values of the control parameter a

Period-doubling is a phenomenon in nonlinear dynamic systems where the period (the time it takes for the system to repeat its behavior) doubles as a control parameter is varied [28]-[29]. This phenomenon is often observed in chaotic systems and is a type of bifurcation, which represents a qualitative change in the system's behavior as a parameter is adjusted. The presented bifurcation diagram in Figure 1 showcases that the system undergoes successive period-doubling phenomena as the parameter a increases. This leads to the familiar period-doubling route to chaos (period-1 \rightarrow period-2 \rightarrow period-4 \rightarrow period-8 \rightarrow chaos) within specific ranges of the parameter a .

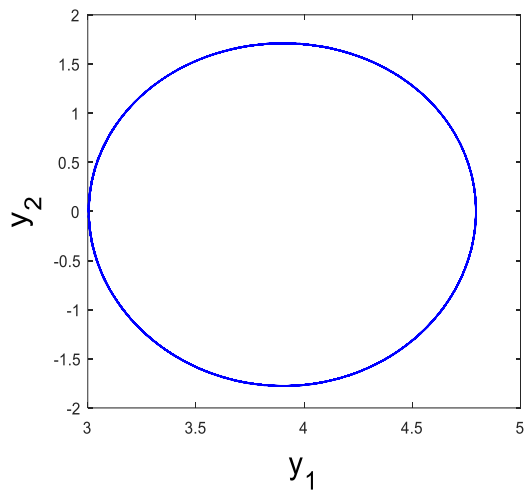
For values of a ranging from 4 to 4.27, the system manifests a period-1 attractor. In the interval between 4.27 and 6.73, a period-2 attractor emerges. Within the

range of 6.73 to 6.83, the system (1) displays a period-4 attractor. Moving further to the interval of 6.83 to 6.86, a period-8 attractor is observed. When a falls within the range of 6.86 to 7.04, the system exhibits a chaotic attractor, marking the end of the period-doubling cascade.

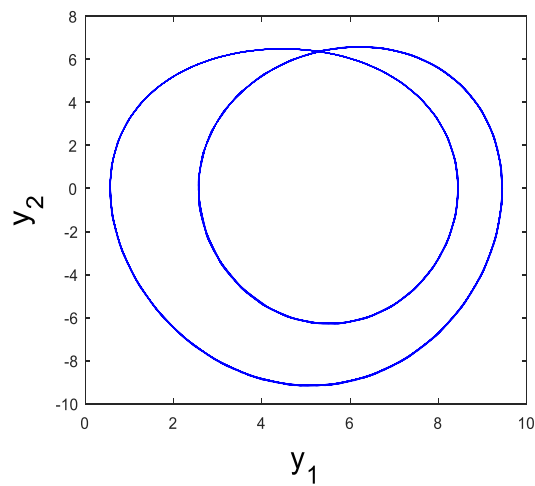
Table 1 encapsulates a summary of the diverse attractors observed in numerical simulations, showcasing the period-doubling route to chaos discussed earlier. Furthermore, Figure 3 offers a visual representation of these attractors.

Table 1. Period-doubling route to chaos with parameter a varying

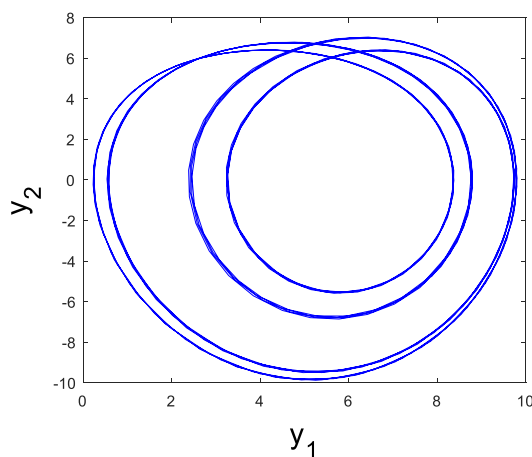
Parameter a range	Parameter a value	Dynamics	Attractor
[4, 4.27]	4	Period-1	Fig. 3(a)
[4.27, 6.73]	6.6	Period-2	Fig. 3(b)
[6.73, 6.83]	6.8	Period-4	Fig. 3(c)
[6.83, 6.86]	6.85	Period-8	Fig. 3(d)
[6.86, 7.04]	6.9	Chaos	Fig. 3(e)



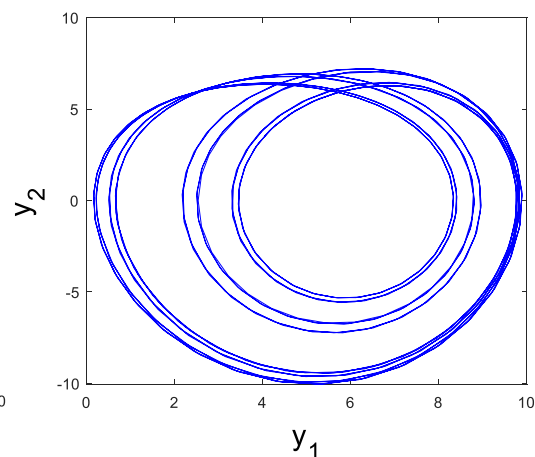
(a)



(b)



(c)



(d)

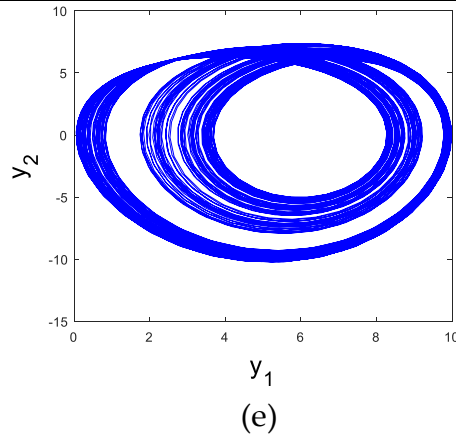


Fig 3: (a): Period-1 for $a = 4$, (b): Period-2 for $a = 6.6$, (c): Period-4 for $a = 6.8$, (d): Period-8 for $a = 6.85$, (e): chaos for $a = 6.9$.

3.5 Parameter b varying

In order to investigate the impact of changes in b on system (1), a is maintained at a constant value of 7.5, while b is systematically adjusted from 3.8 to 5. The Lyapunov exponent spectrum and the bifurcation diagram of system (1) are depicted in Fig. 4. These visuals suggest that as b increases within this range, the system (1) can demonstrate both periodic and chaotic behavior.

System (1) exhibits chaotic behavior, as shown in Figure 5(a), with a single positive Lyapunov exponent when b falls within the intervals of $[3.8, 3.805]$, $[3.810, 3.950]$, $[3.960, 3.995]$, and $[4.025, 4.11]$. The Lyapunov exponents for the system are $LE_1 = 0.152$, $LE_2 = 0$, and $LE_3 = -1.154$ when $b = 3.90$. Furthermore, the system's Kaplan-Yorke dimension is $D_K = 2.1317$, indicating a fractional value.

When b is in the intervals $[3.805, 3.810]$, $[3.950, 3.960]$, $[3.995, 4.025]$, and $[4.11, 5]$, system (1) displays periodic behavior, as illustrated in Figure 5(b). This is marked by one Lyapunov exponent being zero, and the other two being negative. Specifically, for $b = 4.6$, the associated Lyapunov exponent values are: $LE_1 = 0$, $LE_2 = -0.110$, and $LE_3 = -0.893$.

Additionally, the bifurcation diagram presented in Fig. 4 indicates that system (1) undergoes the familiar reverse period-doubling route.

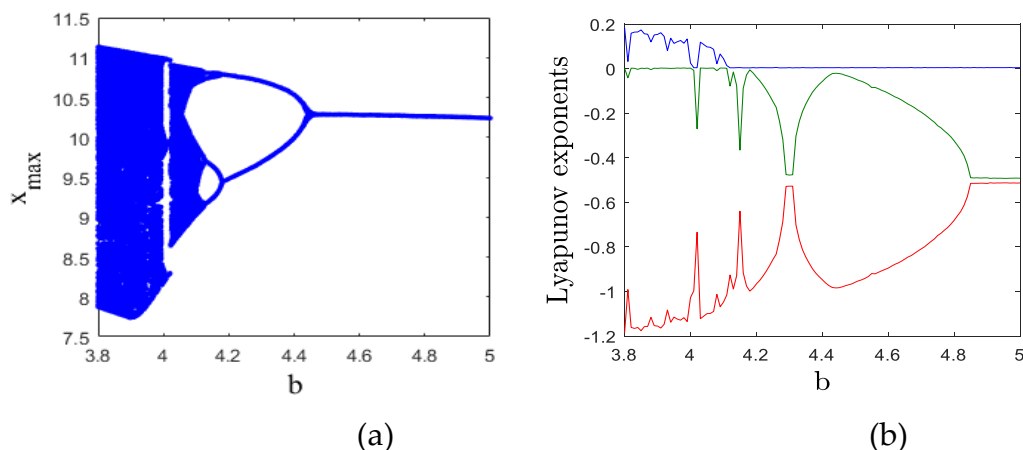


Fig 4: Bifurcation diagram (a) and Lyapunov exponents spectrum

(b) of the supply chain system (1) when: $a=2.3$, $c=0.05$, and $b \in [3.8, 5]$.

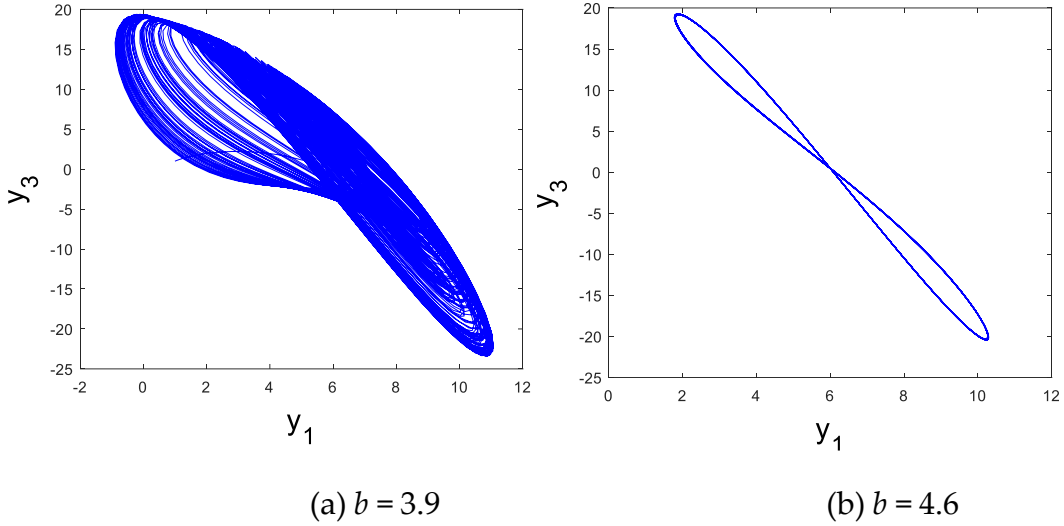


Fig. 5. Phase plots of system (1) for specific values of the control parameter b

The reverse period-doubling route refers to a phenomenon in nonlinear dynamics where a dynamic system undergoes a sequence of bifurcations that lead to the reduction of the period of oscillations rather than an increase [30]. In a standard period-doubling bifurcation, the period of oscillations doubles as a control parameter is varied, leading to a sequence like 1, 2, 4, 8, etc. In the reverse period-doubling route, the system experiences bifurcations that result in halving the period of oscillations.

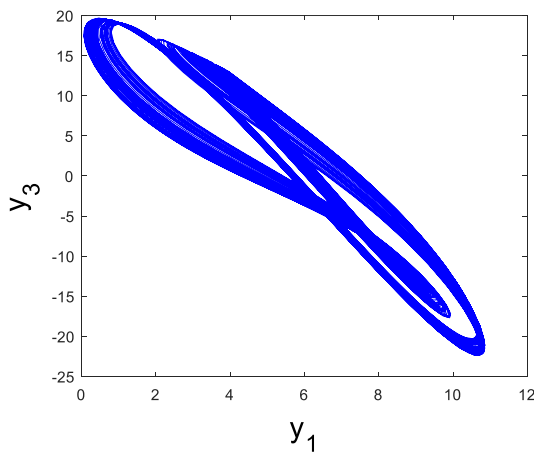
The diagram in Fig. 4 depicts that the system undergoes a sequence of reverse period-doubling bifurcations with increasing values of the parameter b . Consequently, within specific intervals of b , the noteworthy phenomenon of reverse period-doubling unfolds. In this process, the system transitions from chaos to period-16, period-8, period-4, period-2, and ultimately to period-1.

The values assigned to the parameter b exert a noteworthy influence on the system's behavior. For instance, when b spans from 4.025 to 4.11, the system displays a chaotic attractor. At $b = 4.1125$, a period-16 attractor is observed. Similarly, a period-8 attractor occurs when b lies within the range of 4.1125 and 4.125, a period-4 attractor from 4.125 to 4.180, a period-2 attractor between 4.18 and 4.45, and a period-1 attractor from 4.45 to 5, marking the end of the reverse period-doubling route.

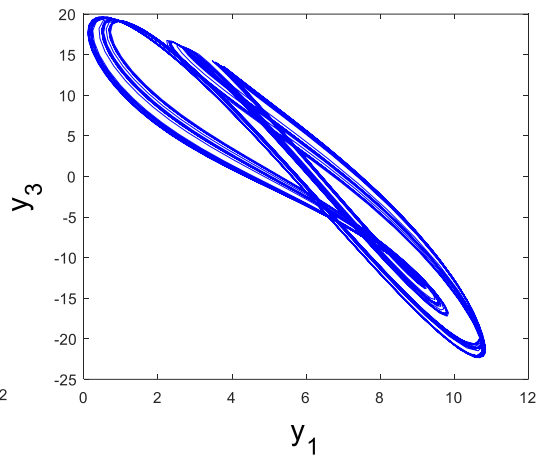
Table 2 provides a detailed listing of the various attractors derived from numerical simulations, illustrating the reverse period-doubling route discussed earlier. Additionally, Fig. 6 offers a visual depiction of these attractors.

Table 2. Revers period-doubling route with parameter b varying

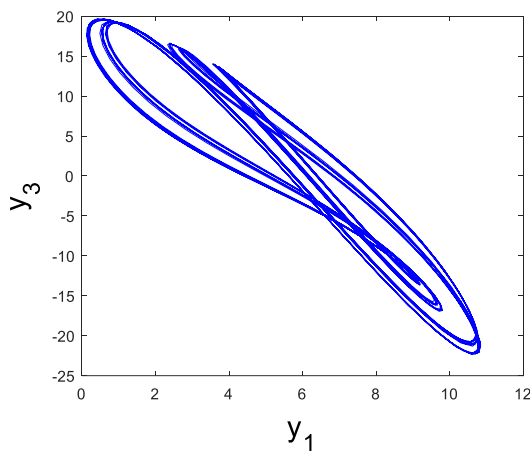
Parameter b range	Parameter b value	Dynamics	Attractor
[4.025, 4.11]	4.10	Chaos	Fig. 6(a)
[4.110, 4.1125]	4.1125	Period-16	Fig. 6(b)
[4.1125, 4.125]	4.12	Period-8	Fig. 6(c)
[4.125, 4.180]	4.15	Period-4	Fig. 6(d)
[4.18, 4.45]	4.25	Period-2	Fig. 6(e)
[4.45, 5]	5	Period-1	Fig. 6(f)



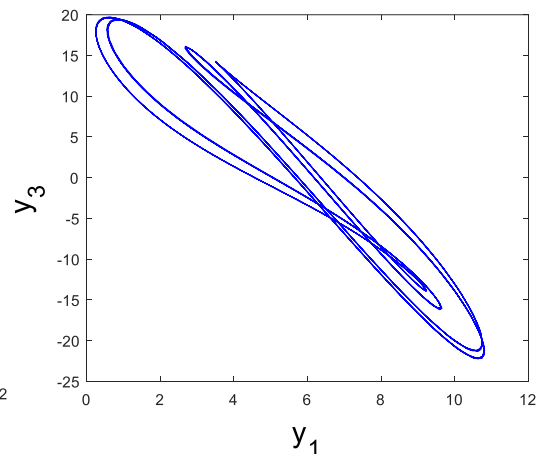
(a)



(b)



(c)



(d)

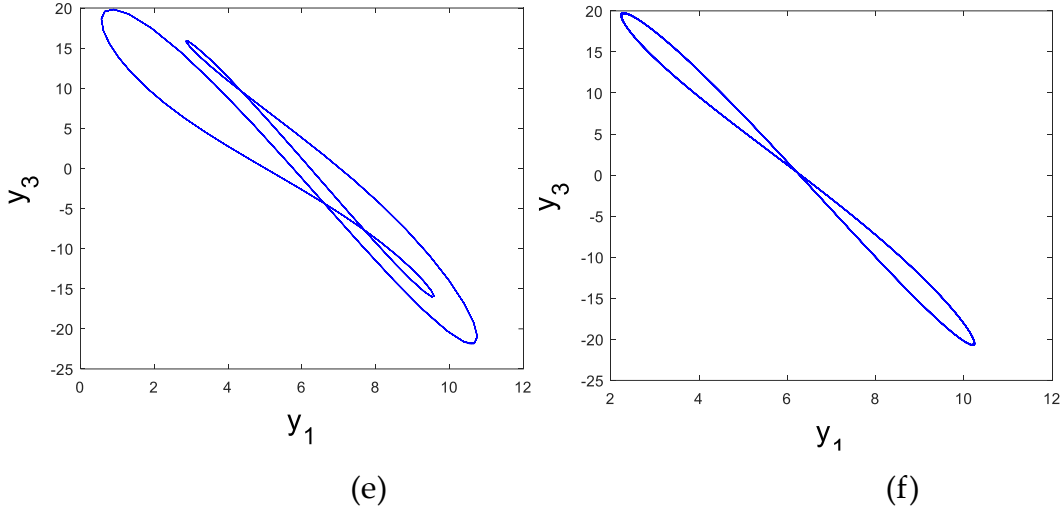


Fig 6: (a): Chaos for $b = 4.10$, (b): Period-16 for $b = 4.1125$, (c): Period-8 for $b = 4.12$, (d): Period-4 for $b = 4.15$, (e): Period-2 for $b = 4.25$, (f): Period-1 for $b = 5$.

3.6 Complete Synchronization of Chaotic SCMM using Backstepping Control

In control systems engineering, backstepping control is a recursive method using Lyapunov stability theory, and this method is very effective for controlling nonlinear dynamical systems in strict-feedback form such as the jerk systems and hyperjerk systems. Backstepping control method has many applications in areas such as robotics, power systems, flight control systems, mechanical oscillators, biological systems, and supply chain models [31].

In view of the special structure of the dynamics for the chaotic supply chain system (1), we use backstepping control method for the complete synchronization of a pair of chaotic supply chain models regarded as the *leader* and *follower* systems.

The leader system is depicted by the chaotic supply chain system with the dynamics

$$\begin{cases} \dot{y}_1 = y_2 \\ \dot{y}_2 = y_3 \\ \dot{y}_3 = ay_1 - by_2 - y_3 - y_1^2 \end{cases} \quad (3)$$

It is noted that the leader system (3) has the same dynamics as the chaotic supply chain system (1).

In the chaotic supply chain system (3), the system states y_1 , y_2 , and y_3 represent the retailers, distributors and manufacturers, respectively.

The follower system is depicted by the chaotic supply chain system with the dynamics

$$\begin{cases} \dot{z}_1 = z_2 \\ \dot{z}_2 = z_3 \\ \dot{z}_3 = az_1 - bz_2 - z_3 - z_1^2 + v \end{cases} \quad (4)$$

In the chaotic supply chain system (4), the system states z_1 , z_2 , and z_3 represent the retailers, distributors, and manufacturers, respectively. Also, v is an active backstepping control which is to be designed using the recursive design procedure given in the backstepping control theory [31].

The synchronization error between the chaotic supply chain systems (4) and (4) can be mathematically defined by means of the following equations:

$$\varepsilon_j = z_j - y_j, \quad (j=1,2,3) \quad (5)$$

By performing a simple mathematical calculation, we derive the dynamics for the synchronization error as given below:

$$\begin{cases} \dot{\varepsilon}_1 = \varepsilon_2 \\ \dot{\varepsilon}_2 = \varepsilon_3 \\ \dot{\varepsilon}_3 = a\varepsilon_1 - b\varepsilon_2 - \varepsilon_3 - z_1^2 + y_1^2 + v \end{cases} \quad (6)$$

In this control section, we shall use Lyapunov stability theory [32] to prove the following main result for the complete synchronization between the chaotic supply chain systems (3) and (4). The chaotic supply chain systems (3) and (4) are said to be completely synchronized if the synchronization error between their respective states converges to zero asymptotically for all values of initial conditions of the chaotic supply chain systems (3) and (4), *i.e.* $\varepsilon_i(t) \rightarrow 0$ as $t \rightarrow \infty$ for all values of $\varepsilon_i(0) \in R$, where $i=1,2,3$.

Theorem 1. The chaotic supply chain systems given by the equations (3) and (4) can be completely synchronized for all initial states $y(0), z(0) \in R^3$ by means of implementing the backstepping control law given by

$$v = -(3+a)\varepsilon_1 - (5-b)\varepsilon_2 - 2\varepsilon_3 + z_1^2 - y_1^2 - L\varphi_3 \quad (7)$$

where the feedback gain $L > 0$ and $\varphi_3 = 2\varepsilon_1 + 2\varepsilon_2 + \varepsilon_3$.

Proof. We establish the result claimed in Theorem 1 using the backstepping control theory [31] and the Lyapunov stability theory [32].

We start the proof by considering the Lyapunov function $W_1(\varphi_1)$ defined by

$$W_1(\varphi_1) = \frac{1}{2}\varphi_1^2 \quad (8)$$

where $\varphi_1 = \varepsilon_1$.

Then it follows immediately that

$$\dot{W}_1(\varphi_1) = \varepsilon_1 \dot{\varepsilon}_1 = \varepsilon_1 \varepsilon_2 = -\frac{1}{2}\varphi_1^2 + \varphi_1 \varphi_2 \quad (9)$$

where $\varphi_2 = \varepsilon_1 + \varepsilon_2$.

Next, we define the Lyapunov function

$$W_2(\varphi_1, \varphi_2) = W_1(\varphi_1) + \frac{1}{2}\varphi_2^2 = \frac{1}{2}\varphi_1^2 + \frac{1}{2}\varphi_2^2 \quad (10)$$

A simple mathematical calculation yield

$$\dot{W}_2(\varphi_1, \varphi_2) = -\frac{1}{2}\varphi_1^2 - \frac{1}{2}\varphi_2^2 + \varphi_2 \varphi_3 \quad (11)$$

where $\varphi_3 = \varepsilon_1 + \varepsilon_2 + \varepsilon_3$.

Finally, we consider the Lyapunov function

$$W(\varphi_1, \varphi_2, \varphi_3) = W_2(\varphi_1, \varphi_2, \varphi_3) + \frac{1}{2}\varphi_3^2 = \frac{1}{2}\varphi_1^2 + \frac{1}{2}\varphi_2^2 + \frac{1}{2}\varphi_3^2 \quad (12)$$

Clearly, W is a quadratic and positive definite function defined on R^3 . Moreover,

$$\dot{W} = \dot{W}_2 + \varphi_3 \dot{\varphi}_3 = -\varphi_1^2 - \varphi_2^2 - \varphi_3^2 + \varphi_3 Z, \quad (13)$$

where,

$$Z = \varphi_2 + \varphi_3 + \dot{\varphi}_3 = (3+a)\varepsilon_1 + (5-b)\varepsilon_2 + 2\varepsilon_3 - z_1^2 + y_1^2 + \nu \quad (14)$$

Substituting the definition for ν from Eq. (7) into Eq. (14), we get $Z = -L\varphi_3$.

Then Eq. (13) can be simplified as follows:

$$\dot{W} = -\varphi_1^2 - \varphi_2^2 - (1+L)\varphi_3^2 \quad (15)$$

which is negative definite everywhere on R^3 .

Using Lyapunov stability theory [32], we conclude that the synchronization error dynamics (6) is globally asymptotically stable for all initial values of the synchronization error.

This completes the proof. ■

We present MATLAB simulations for the synchronization result in Theorem 1. We choose the parameters of the chaotic supply chain systems (3) and (4) as $a = 7.5$, and $b = 3.8$. We let $L = 12$. We choose the initial state of the chaotic supply chain system (3) as $y(0) = (1.6, 4.5, 2.1)$, and the initial state of the chaotic supply chain system (4) as $z(0) = (5.1, 2.3, 0.6)$.

Figure 1 shows the asymptotic convergence of the synchronization errors ($\varepsilon_1(t), \varepsilon_2(t), \varepsilon_3(t)$) between the chaotic supply chain systems (3) and (4).

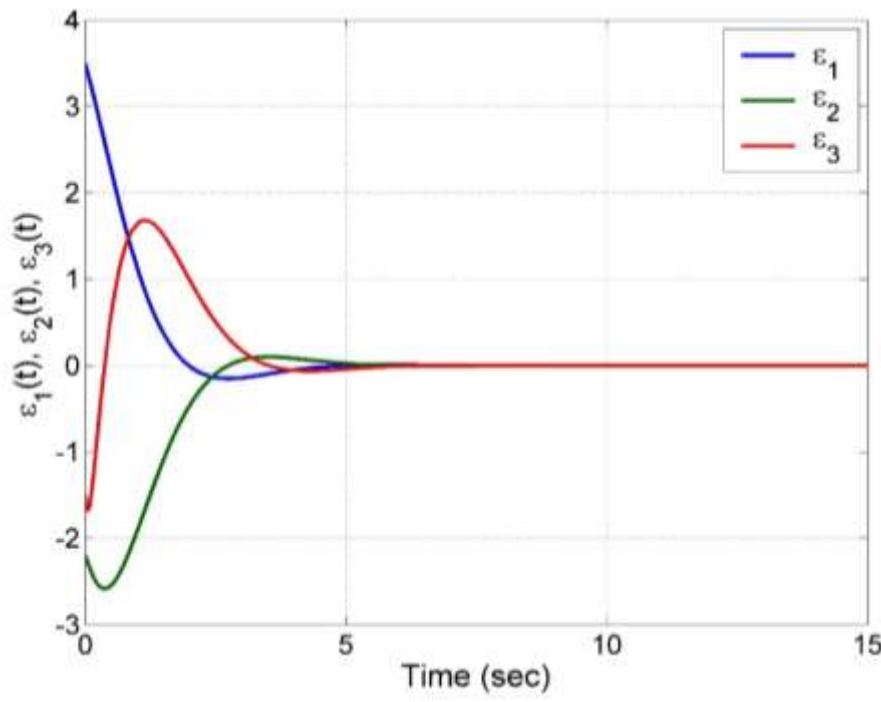


Figure 7. Time-history of the synchronization error between the supply chain systems (3) and (4)

with $y(0) = (1.6, 4.5, 2.1)$ and $z(0) = (5.1, 2.3, 0.6)$.

3.7 Conclusion

In conclusion, this study has delved into the intricate dynamics and complexity within the supply chain mathematical model (SCMM) developed by Hamidzadeh et al. (2023) through the lens of bifurcation analysis. Bifurcation points, serving as critical thresholds in chaotic systems, have been examined to understand the qualitative shifts in behavior, particularly within the context of supply chains. The primary objective of this investigation was to scrutinize the stability of the SCMM. Our analysis revealed significant bifurcation phenomena, including Hopf bifurcation, transcritical bifurcation, and double-zero bifurcation. These findings contribute to a deeper understanding of the structural changes that can occur within the

SCMM, potentially signifying shifts in demand patterns, material flow disruptions, or alterations in market conditions.

Furthermore, the exploration extended to the dynamical characteristics of the SCMM, utilizing bifurcation diagrams and Lyapunov exponents. The outcomes unveiled a diverse range of behaviors, including periodic, chaotic, and reverse period-doubling, underscoring the complexity inherent in supply chain dynamics. To manage the chaotic nature of the SCMM, backstepping controllers were employed, demonstrating their effectiveness in achieving synchronization between two SCMMs. This strategic application of control methodologies opens avenues for enhancing the stability and coordination of supply chain systems. Numerical simulations were conducted to provide empirical evidence of the practical applicability and effectiveness of the proposed methodologies. The results validate the robustness of the backstepping controllers in taming chaotic SCMM behavior, offering a promising approach for real-world implementation. In essence, this study contributes valuable insights into the dynamics of supply chain systems, emphasizing the significance of bifurcation analysis and control strategies. The methodologies explored herein not only enhance our theoretical understanding but also offer practical solutions for managing the complexities of SCMM in dynamic and unpredictable environments.

3.8 References

- [1] Hmioui, A., & Bentalha, B. (2021). Service supply chain management: a literature review. *International Journal of Logistics Systems and Management*, 40(3), 332-353.
- [2] Akam, M. J., Sunday, E. G., Etuk, I. U., Ejikeme, O. B., & Arikpo, N. N. (2023). The role of integrated coordination in supply chain performance of firms in the manufacturing industry. *International Journal of Integrated Supply Management*, 16(1), 26-51.
- [3] Abdallah, A. B., Alfar, N. A., & Alhyari, S. (2021). The effect of supply chain quality management on supply chain performance: the indirect roles of supply chain agility and innovation. *International Journal of Physical Distribution & Logistics Management*, 51(7), 785-812.
- [4] Sundram, V. P. K., Chhetri, P., & Bahrin, A. S. (2020). The consequences of information technology, information sharing and supply chain integration, towards supply chain performance and firm performance. *Journal of International Logistics and Trade*, 18(1), 15-31.
- [5] Li, J., Chen, C. W., Wu, C. H., Hung, H. C., & Lin, C. T. (2020). How do partners benefit from IT use in supply-chain management: An empirical study of Taiwan's bicycle industry. *Sustainability*, 12(7), 2883.
- [6] Das, S., & Hassan, H. K. (2022). Impact of sustainable supply chain management and customer relationship management on organizational performance. *International Journal of Productivity and Performance Management*, 71(6), 2140-2160.
- [7] Xu, X., Lee, S. D., Kim, H. S., & You, S. S. (2021). Management and optimisation of chaotic supply chain system using adaptive sliding mode control algorithm. *International journal of production research*, 59(9), 2571-2587.
- [8] Kocamaz, U. E., Taşkın, H., Uyaroğlu, Y., & Göksu, A. (2016). Control and synchronization of chaotic supply chains using intelligent approaches. *Computers & Industrial Engineering*, 102, 476-487.
- [9] Göksu, A., Kocamaz, U. E., & Uyaroğlu, Y. (2015). Synchronization and control of chaos in supply chain management. *Computers & Industrial Engineering*, 86, 107-115.

-
- [10] Nav, H. N., Motlagh, M. R. J., & Makui, A. (2018). Modeling and analyzing the chaotic behavior in supply chain networks: A control theoretic approach. *Journal of Industrial & Management Optimization*, 14(3), 1123-1141.
- [11] Açıkgöz, N., Çağıl, G., & Uyaroğlu, Y. (2020). The experimental analysis on safety stock effect of chaotic supply chain attractor. *Computers & Industrial Engineering*, 150, 106881.
- [12] Chen, X., & Zhou, J. (2021). The complexity analysis and chaos control in omnichannel supply chain with consumer migration and advertising cost sharing. *Chaos, Solitons & Fractals*, 146, 110884.
- [13] Tian, Y., Ma, J., Xie, L., Koivumäki, T., & Seppänen, V. (2020). Coordination and control of multi-channel supply chain driven by consumers' channel preference and sales effort. *Chaos, Solitons & Fractals*, 132, 109576.
- [14] Peng, Y., Wu, J., Wen, S., Feng, Y., Tu, Z., & Zou, L. (2020). A new supply chain system and its impulsive synchronization. *Complexity*, 2020, 1-9.
- [15] Qian, Y., Yu, X. A., Shen, Z., & Song, M. (2023). Complexity analysis and control of game behavior of subjects in green building materials supply chain considering technology subsidies. *Expert Systems with Applications*, 214, 119052.
- [16] Han, W., & Wang, J. (2015). The impact of cooperation mechanism on the chaotic behaviours in nonlinear supply chains. *European Journal of Industrial Engineering*, 9(5), 595-612.
- [17] Wang, B., Jahanshahi, H., Volos, C., Bekiros, S., Yusuf, A., Agarwal, P., & Aly, A. A. (2021). Control of a symmetric chaotic supply chain system using a new fixed-time super-twisting sliding mode technique subject to control input limitations. *Symmetry*, 13(7), 1257.
- [18] Nav, H. N., Jahedmotlagh, M. R., & Makui, A. (2017). Robust H^∞ control for chaotic supply chain networks. *Turkish Journal of Electrical Engineering and Computer Sciences*, 25(5), 3623-3636.
- [19] Mondal, S. (2019). A new supply chain model and its synchronization behaviour. *Chaos, Solitons & Fractals*, 123, 140-148.

-
- [20] Lei, Z., Li, Y. J., & Xu, Y. Q. (2006, October). Chaos synchronization of bullwhip effect in a supply chain. In 2006 international conference on management science and engineering (pp. 557-560). IEEE.
- [21] Yan, L., Liu, J., Xu, F., Teo, K. L., & Lai, M. (2021). Control and synchronization of hyperchaos in digital manufacturing supply chain. *Applied mathematics and computation*, 391, 125646.
- [22] Hamidzadeh, S. M., Rezaei, M., & Ranjbar-Buorani, M. (2022). Control and Synchronization of The Hyperchaotic Closedloop Supply Chain Network by PI Sliding Mode Control. *International Journal of Industrial Engineering & Production Research*, 33(4), 1-13.
- [23] Liu, Z., Jahanshahi, H., Gómez-Aguilar, J. F., Fernandez-Anaya, G., Torres-Jiménez, J., Aly, A. A., & Aljuaid, A. M. (2021). Fuzzy adaptive control technique for a new fractional-order supply chain system. *Physica Scripta*, 96(12), 124017.
- [24] Lou, W., Ma, J., & Zhan, X. (2017). Bullwhip entropy analysis and chaos control in the supply chain with sales game and consumer returns. *Entropy*, 19(2), 64.
- [25] Alsaadi, F. E., Bekiros, S., Yao, Q., Liu, J., & Jahanshahi, H. (2023). Achieving resilient chaos suppression and synchronization of fractional-order supply chains with fault-tolerant control. *Chaos, Solitons & Fractals*, 174, 113878.
- [26] Hamidzadeh, S. M., Rezaei, M., & Ranjbar-Bourani, M. (2023). Chaos synchronization for a class of uncertain chaotic supply chain and its control by ANFIS. *International Journal of Production Management and Engineering*, 11(2), 113-126.
- [27] Lăzureanu, C., & Cho, J. (2023). On Hopf and fold bifurcations of jerk systems. *Mathematics*, 11(20), 4295.
- [28] Sambas, A., Miroslav, M., Vaidyanathan, S., Ovilla-Martínez, B., Tlelo-Cuautle, E., Abd El-Latif, A. A., ... & Bonny, T. (2024). A New Hyperjerk System with a Half Line Equilibrium: Multistability, Period Doubling Reversals, Antimonotonicity, Electronic Circuit, FPGA Design and an Application to Image Encryption. *IEEE Access*, 12, 9177-9194.

[29] Sambas, A., Vaidyanathan, S., Zhang, X., Koyuncu, I., Bonny, T., Tuna, M., ... & Kumam, P. (2022). A novel 3D chaotic system with line equilibrium: multistability, integral sliding mode control, electronic circuit, FPGA implementation and its image encryption. *IEEE Access*, 10, 68057-68074.

[30] Sambas, A., Mohammadzadeh, A., Vaidyanathan, S., Ayob, A. F. M., Aziz, A., Mohamed, M. A., ... & Nawi, M. A. A. (2023). Investigation of chaotic behavior and adaptive type-2 fuzzy controller approach for Permanent Magnet Synchronous Generator (PMSG) wind turbine system. *AIMS Mathematics*, 8(3), 5670-5686.

[31] S. Vaidyanathan and A.T. Azar, *Backstepping Control of Nonlinear Dynamical Systems*, First Edition, Academic Press, New York, USA, 2021. (ISBN: 978-0-12-81752-8)

[32] H. K. Khalil, *Nonlinear Systems*, Third Edition, Pearson, NJ, USA, 2002 (ISBN: 978-0-1306-73893)